IPELS-16@IPP, Garching Aug 5 – 9, 2024

Magnetic Heating during State Transitions in Black Hole Accretion Flows

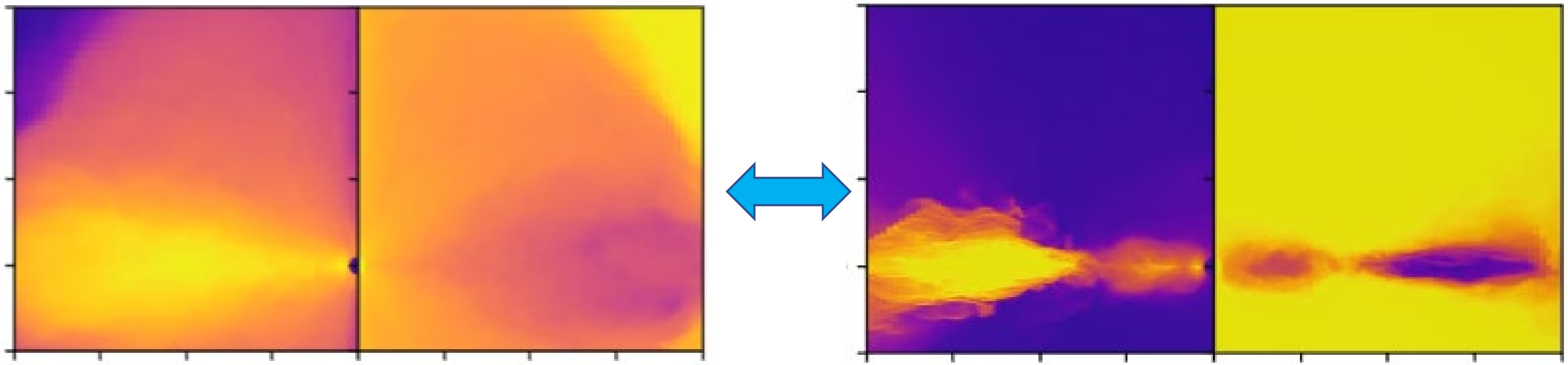

Ryoji Matsumoto (Chiba Univ.)

T. Igarashi (NAOJ/Rikkyo Univ), H.R. Takahashi (Komazawa Univ.),

T. Kawashima (ICRR, Univ. Tokyo), K. Ohsuga (Tsukuba Univ.),

and Y. Matsumoto (Chiba Univ.)

Activities of Black Hole Candidates

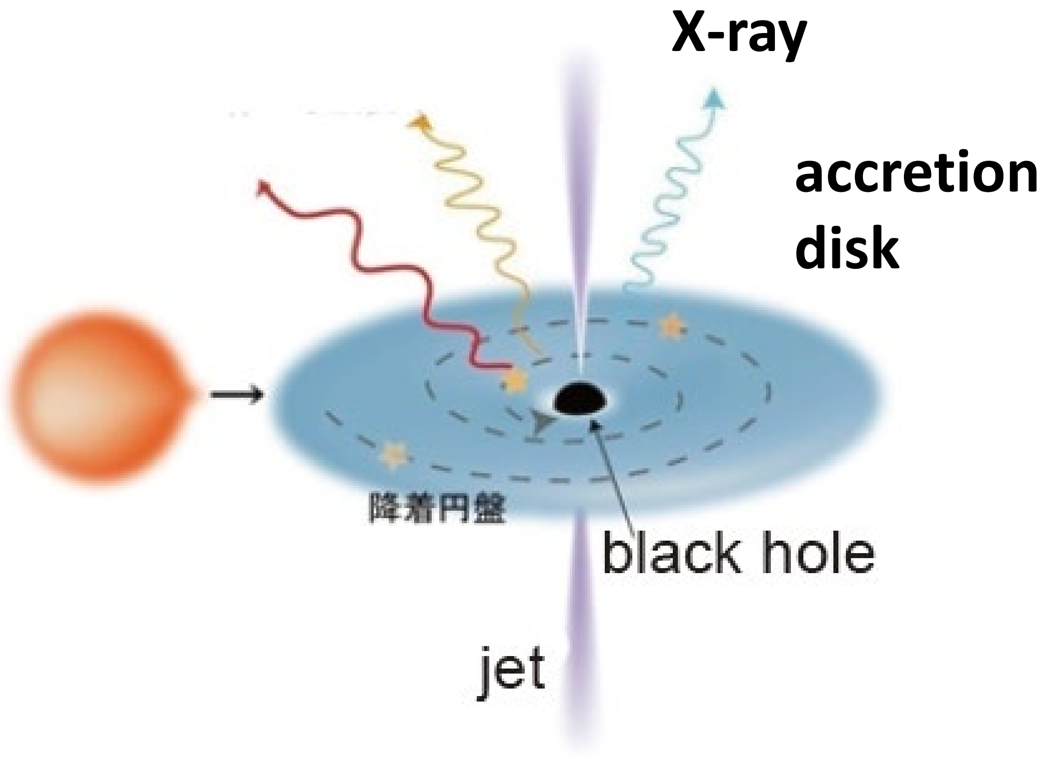

X-ray Binary

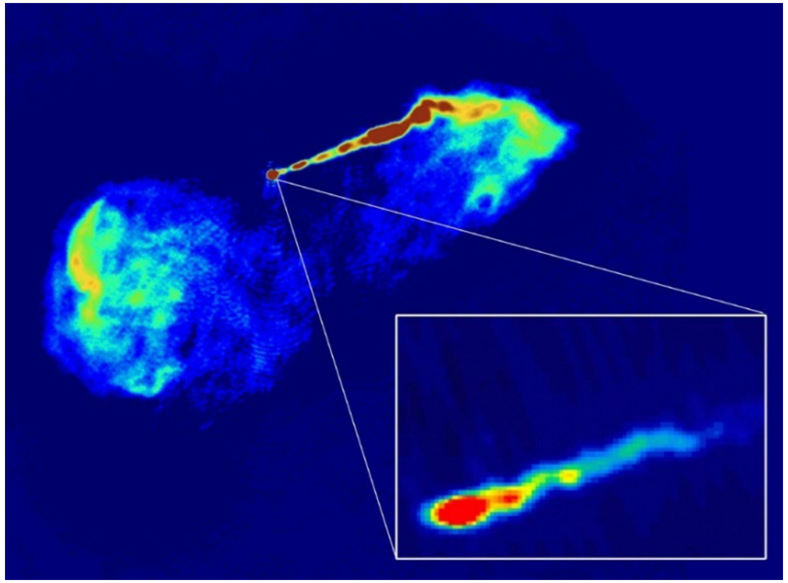

M87

VLA+
HALCA

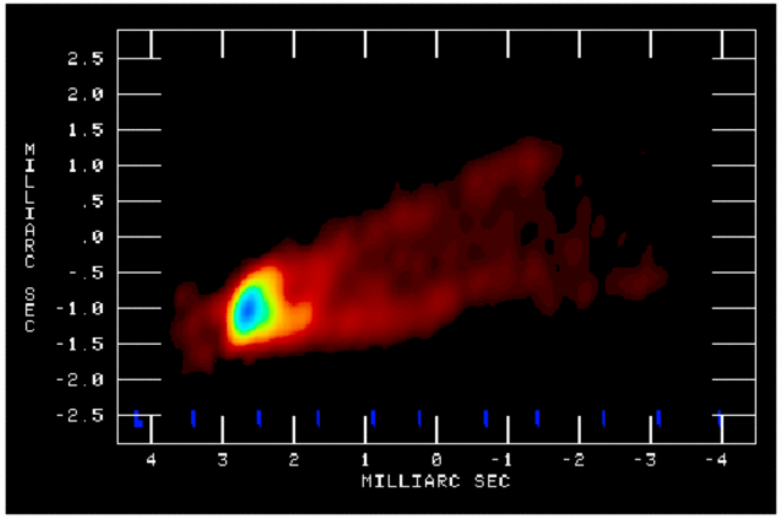

VLBA 43GHz
Walker et al.
2007

Global Three-Dimensional MHD Simulations of Radiatively Inefficient Black Hole Accretion Flows

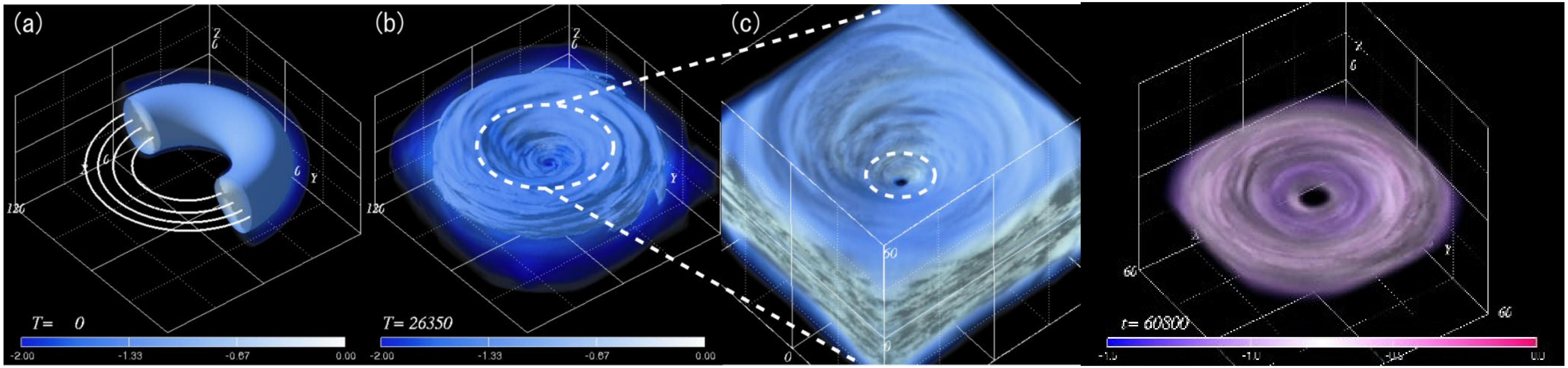

Machida et al. 2003

State Transitions of Black Hole Candidates

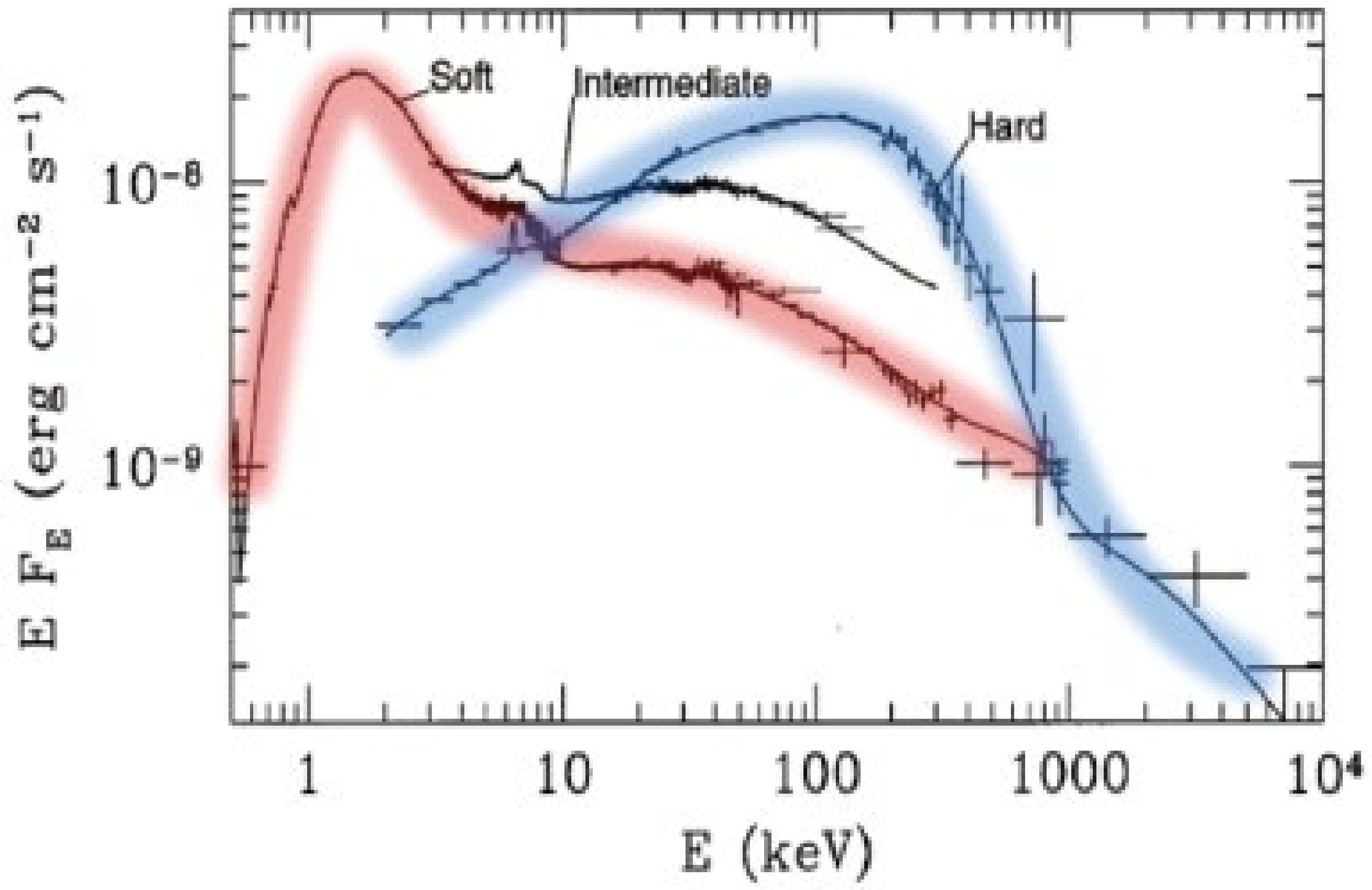

X-ray Spectrum of Cyg X-1（Gierlinski 1999）

Theoretical Model of State Transitions of Black Hole Candidates

$$\dot{M}_{\mathrm{Edd}} = L_{\mathrm{Edd}}/c^2$$

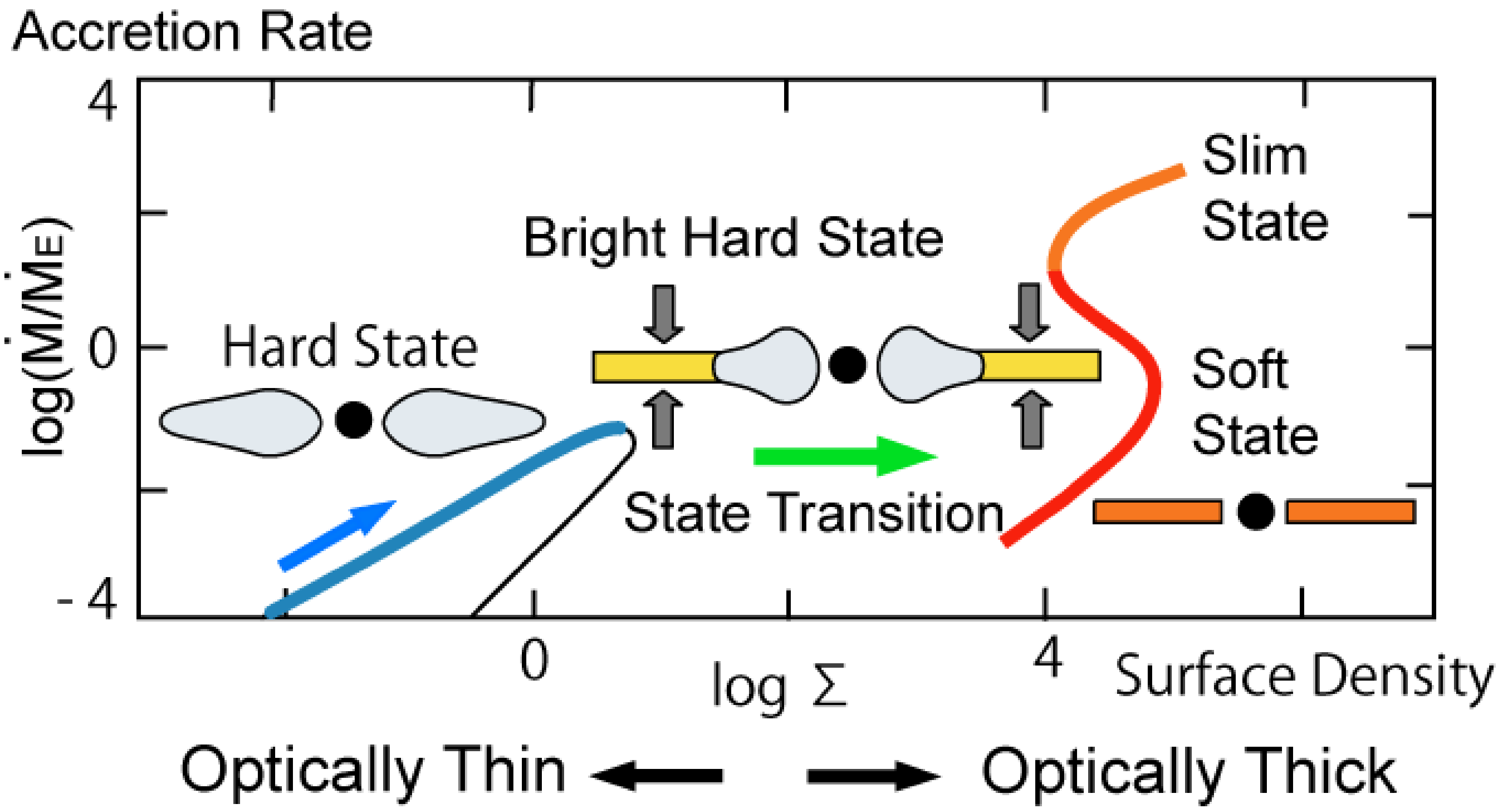

Thermal Equilibrium Curves of Accretion Flows (Abramowicz et al. 1995)

Formation of Magnetically Supported Low-β Disk

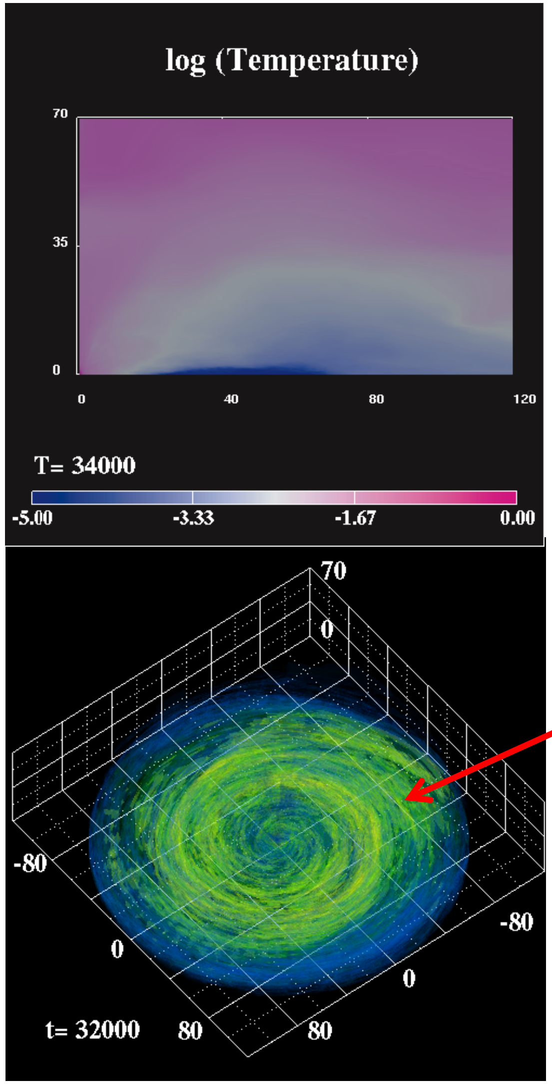

$\beta < 1$

3D MHD Simulation including Cooling

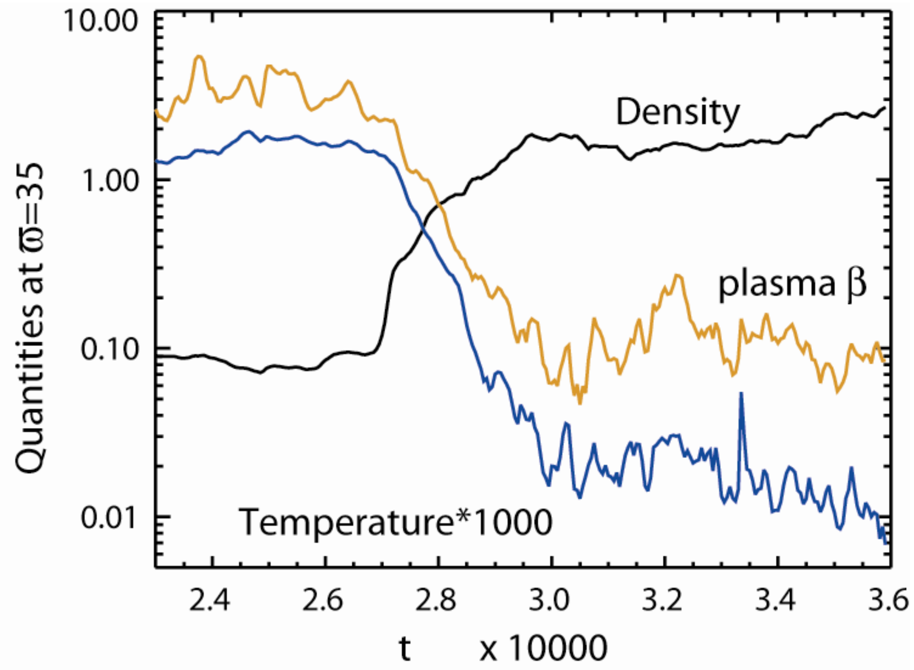

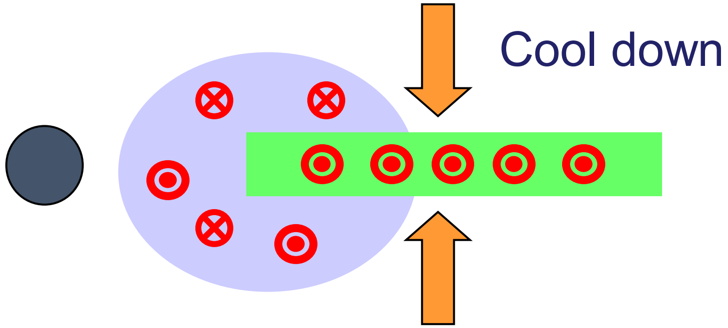

(Machida et al. 2006)

Thermal Equilibrium Curve Considering Toroidal Magnetic Field and Evolution of Accretion Disk

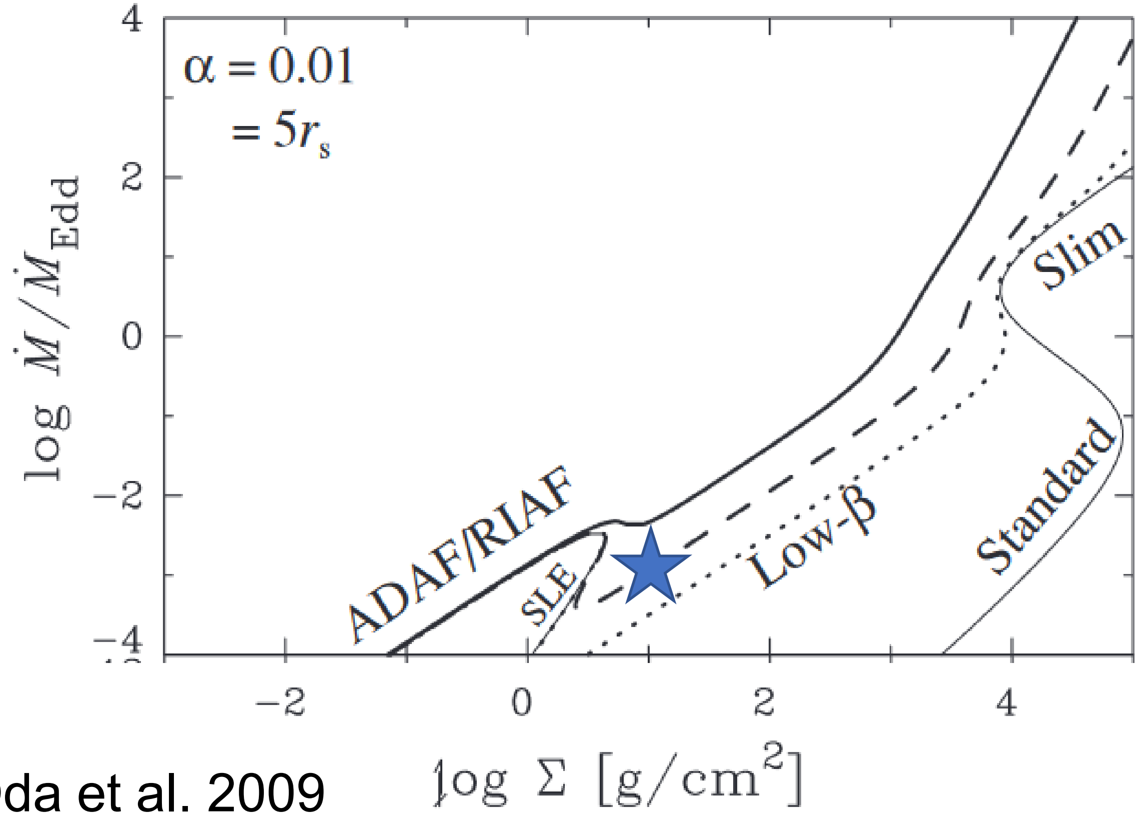

Oda et al. 2009

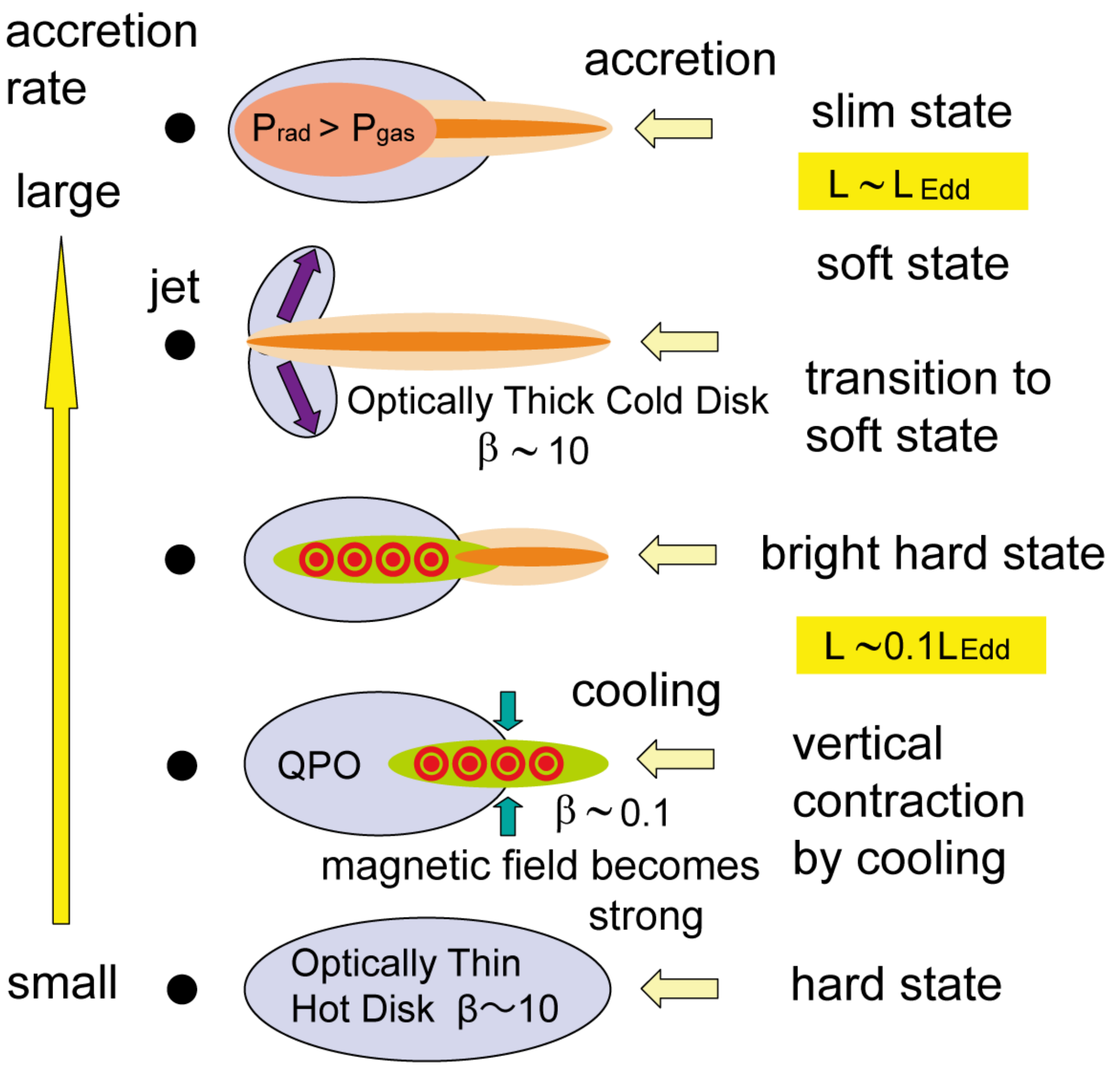

Basic equations of Radiation MHD

MHD

$$\frac{\partial \rho}{\partial t} + \nabla \cdot (\rho \boldsymbol{v}) = 0$$

$$\frac{\partial (\rho \boldsymbol{v})}{\partial t} + \nabla \cdot \left[\rho \boldsymbol{v}\boldsymbol{v} + p_{\mathrm{t}} I - \frac{\boldsymbol{B}\boldsymbol{B}}{4\pi} \right] = -\rho \nabla \phi - \boxed{\boldsymbol{S}}$$

$$\frac{\partial E_{\mathrm{t}}}{\partial t} + \nabla \cdot \left[(E_{\mathrm{t}} + p_{\mathrm{gas}}) \boldsymbol{v} - \frac{\boldsymbol{B}(\boldsymbol{v} \cdot \boldsymbol{B})}{4\pi} \right] = -\rho \boldsymbol{v} \cdot \nabla \phi - \nabla \cdot \left(\frac{4\pi\eta}{c} \boldsymbol{j} \times \boldsymbol{B} \right) - \boxed{cS_0}$$

$$\frac{\partial \boldsymbol{B}}{\partial t} + \nabla \cdot (\boldsymbol{B}\boldsymbol{v} - \boldsymbol{v}\boldsymbol{B}) = -\nabla \times \left(\frac{4\pi\eta}{c} \boldsymbol{j} \right)$$

Pseudo Newtonian potential

$$\phi_{\mathrm{PN}} = -\frac{GM}{R - r_s}$$

Rad. Moment eq

$$\frac{\partial E}{\partial t} + \nabla \cdot \boldsymbol{F} = \boxed{cS_0}$$

$$\frac{1}{c^2} \frac{\partial \boldsymbol{F}}{\partial t} + \nabla \cdot \boldsymbol{P} = \boxed{\boldsymbol{S}}$$

Source term

$$cS_0 = \rho \kappa_{\mathrm{ff}} c (4\pi B(T) - E) + \rho (\kappa_{\mathrm{ff}} - \kappa_{\mathrm{es}}) \frac{\boldsymbol{v}}{c} \cdot [\boldsymbol{F} - (\boldsymbol{v} E + \boldsymbol{v} \cdot \boldsymbol{P})] + \Gamma_{\mathrm{c}}$$

$$\boldsymbol{S} = \rho \kappa_{\mathrm{ff}} \frac{\boldsymbol{v}}{c} (4\pi B(T) - E) - \rho (\kappa_{\mathrm{ff}} + \kappa_{\mathrm{es}}) \frac{1}{c} [\boldsymbol{F} - (\boldsymbol{v} E + \boldsymbol{v} \cdot \boldsymbol{P})]$$

$$\Gamma_{\mathrm{c}} = \rho \kappa_{\mathrm{es}} c E_{\mathrm{r0}} \frac{4 k_{\mathrm{B}} (T_{\mathrm{e}} - T_{\mathrm{r}})}{m_{\mathrm{e}} c^2}$$

Compton Cooling

Electron scattering opacity

$$\kappa_{\mathrm{es}} = \frac{\sigma_{\mathrm{T}}}{m_{\mathrm{p}}} = 0.4$$

Free-free opacity

$$\kappa_{\mathrm{ff}} = 1.7 \times 10^{-25} m_{\mathrm{p}}^{-2} \rho T_{\mathrm{gas}}^{-3.5}$$

Simulation Code : CANS+R　MHD：CANS+(HLLD+MP5) (Matsumoto et al. 2019)

Rad： Non-relativistic version of M1-closure scheme (Takahashi & Ohsuga 2013)

Global 3D Radiation MHD Simulations of Black Hole Accretion Flows during State Transition

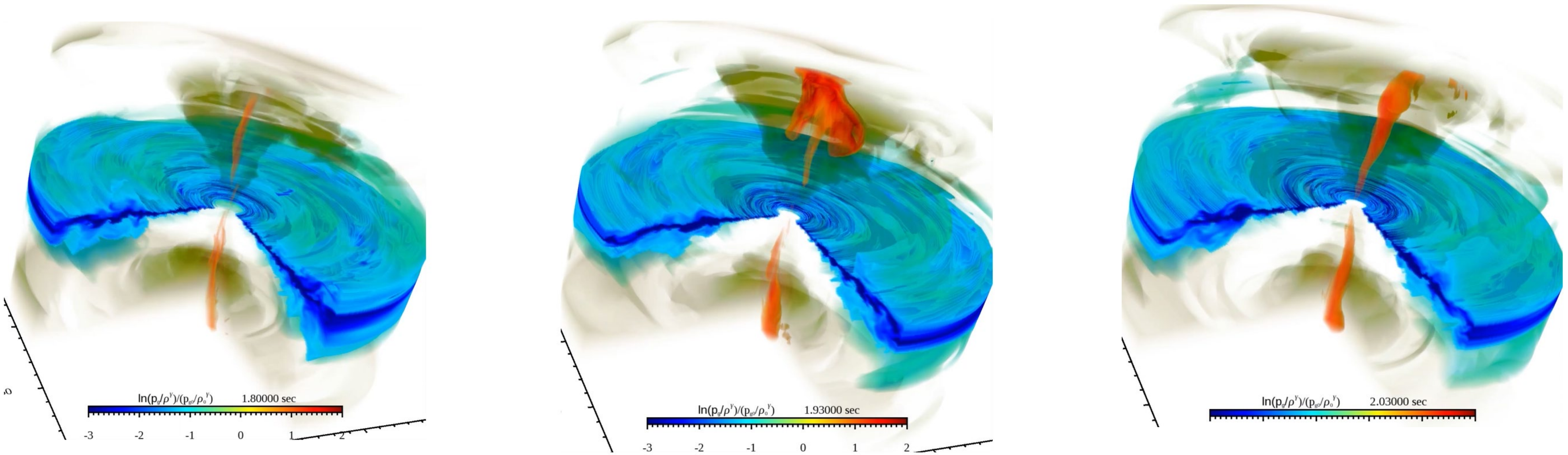

Color: Entropy　(provided by Igarashi）

Radiation MHD simulations of sub-Eddington accretion flows are carried out only recently by Jiang et al. 2019, Igarashi et al. 2020, Dexter et al. 2021, Liska et al. 2022, and Huang et al. 2023

Can We Observe State Change of AGN? Yes !
Changing Look AGNs are Found

Type 1 : Broad emission lines

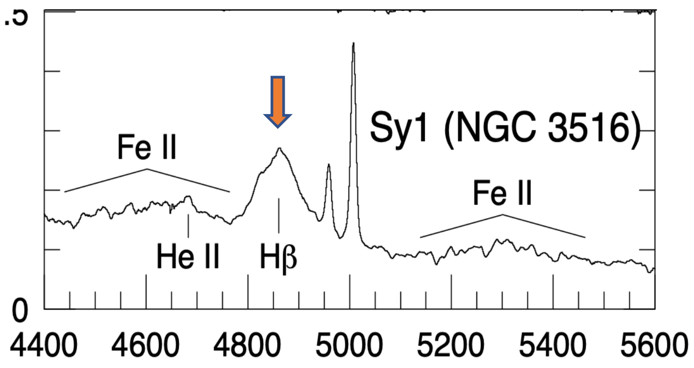

Type 2 : No broad emission lines

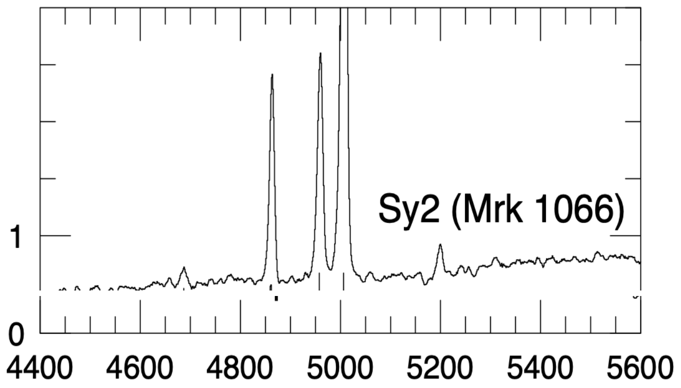

Pogge 2000

State Transitions between type 1 and type 2 are observed

Changing Look AGN

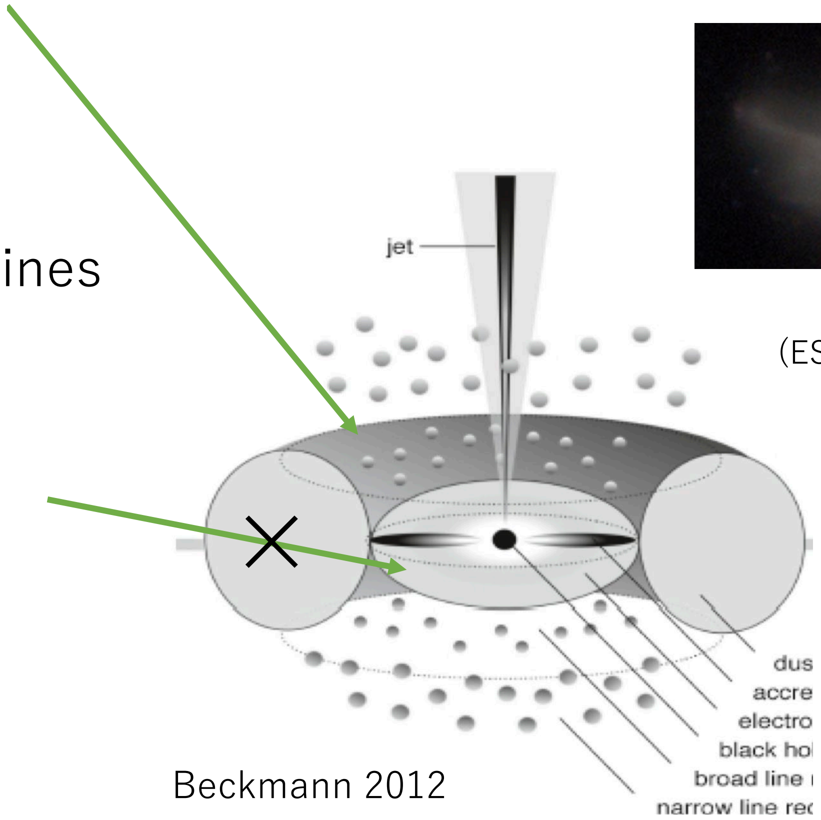

Beckmann 2012

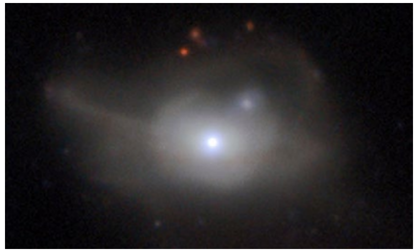

Mrk1018
(ESO/CARS survey)

X-ray Observation Revealed The Spectral Change during State Transition

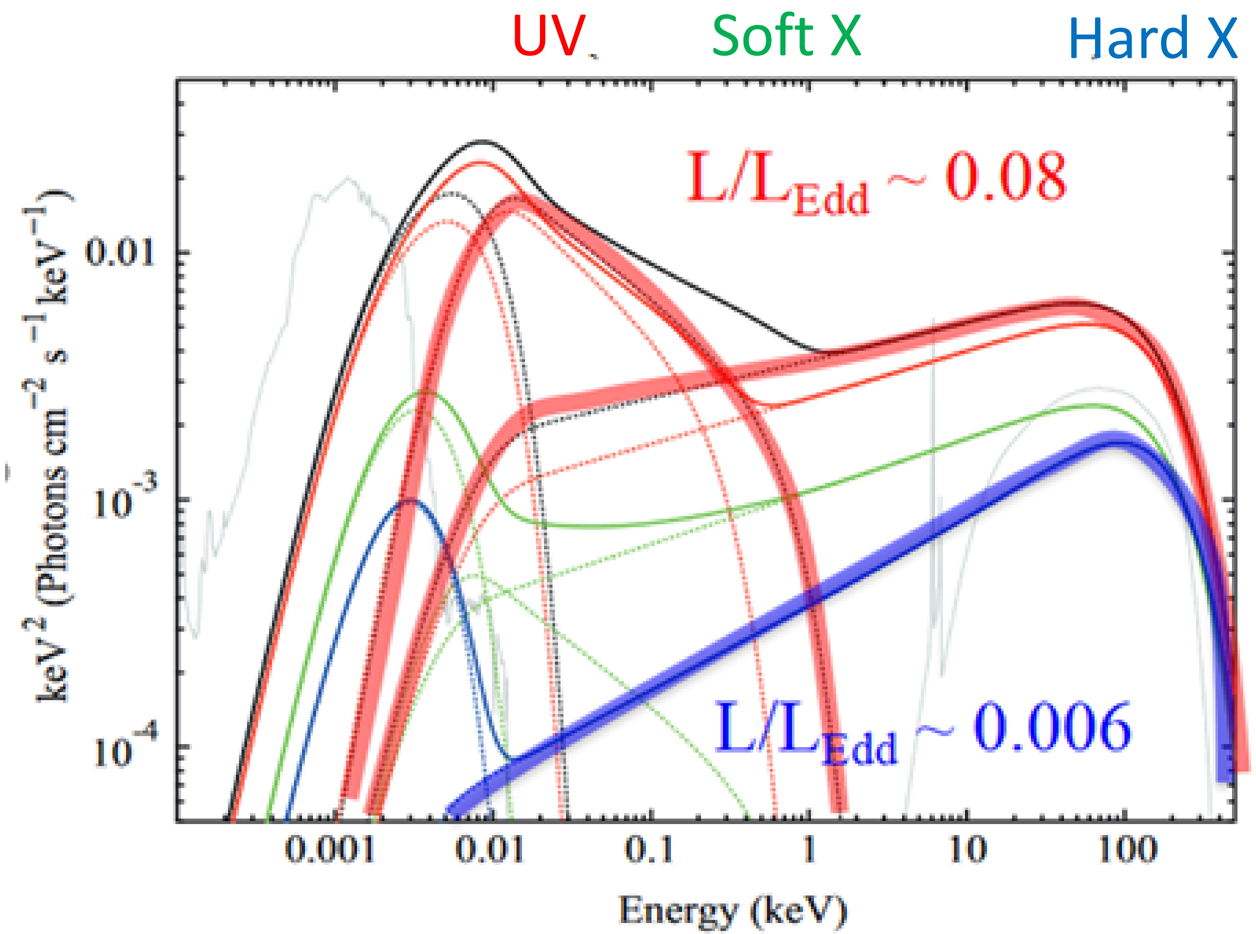

Soft X-ray Excess Appears during State Transition

Similar to the Hard-to-Soft State Transitions of Stellar Mass Black Hole Candidates

Radiation Spectrum of a changing look AGN Mrk1018 (Noda and Done 2018)

Radiation MHD Simulation during Changing Look Phenomena in AGN (Igarashi et al 2024, ApJ 968, 121)

- $M_{BH} = 10^7 M_\odot$
- Unit Length $r_s = 3\times10^{12}$cm
- Unit time $t_0 = r_s/c$ =100sec
- Radiative cooling terms are turned on after RIAF is formed.
- Density is adjusted so that the accretion rate at this state is 10% of the Eddington accretion rate defined by

$$\dot{M}_{\rm Edd} = L_{\rm Edd}/c^2$$

- Number of grid points

  (N_r, N_φ, N_z)=(464.32.464)

  $\Delta r = \Delta z = 0.1 r_s$@ $r < 20$rs, $|z| < 5r_s$

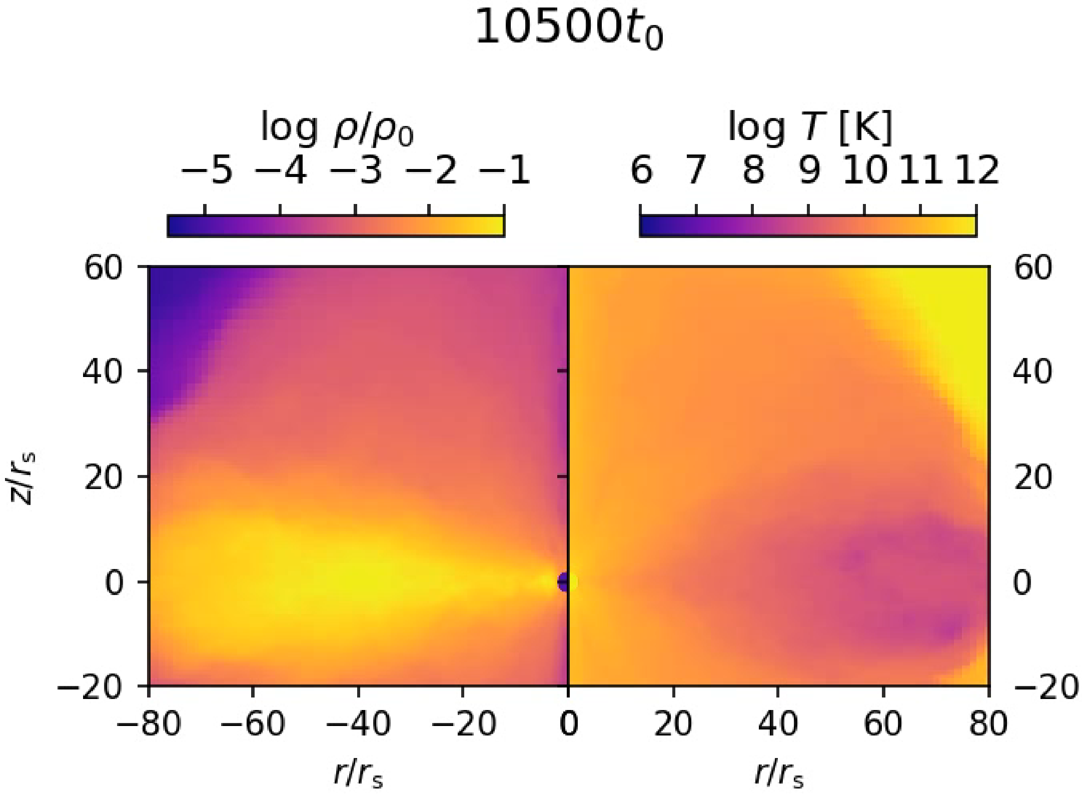

Igarashi et al. 2024, ApJ

Distribution of Density, Temperature, and Radiation Energy Density averaged over $1.5<t/10^4 t_0<1.75$

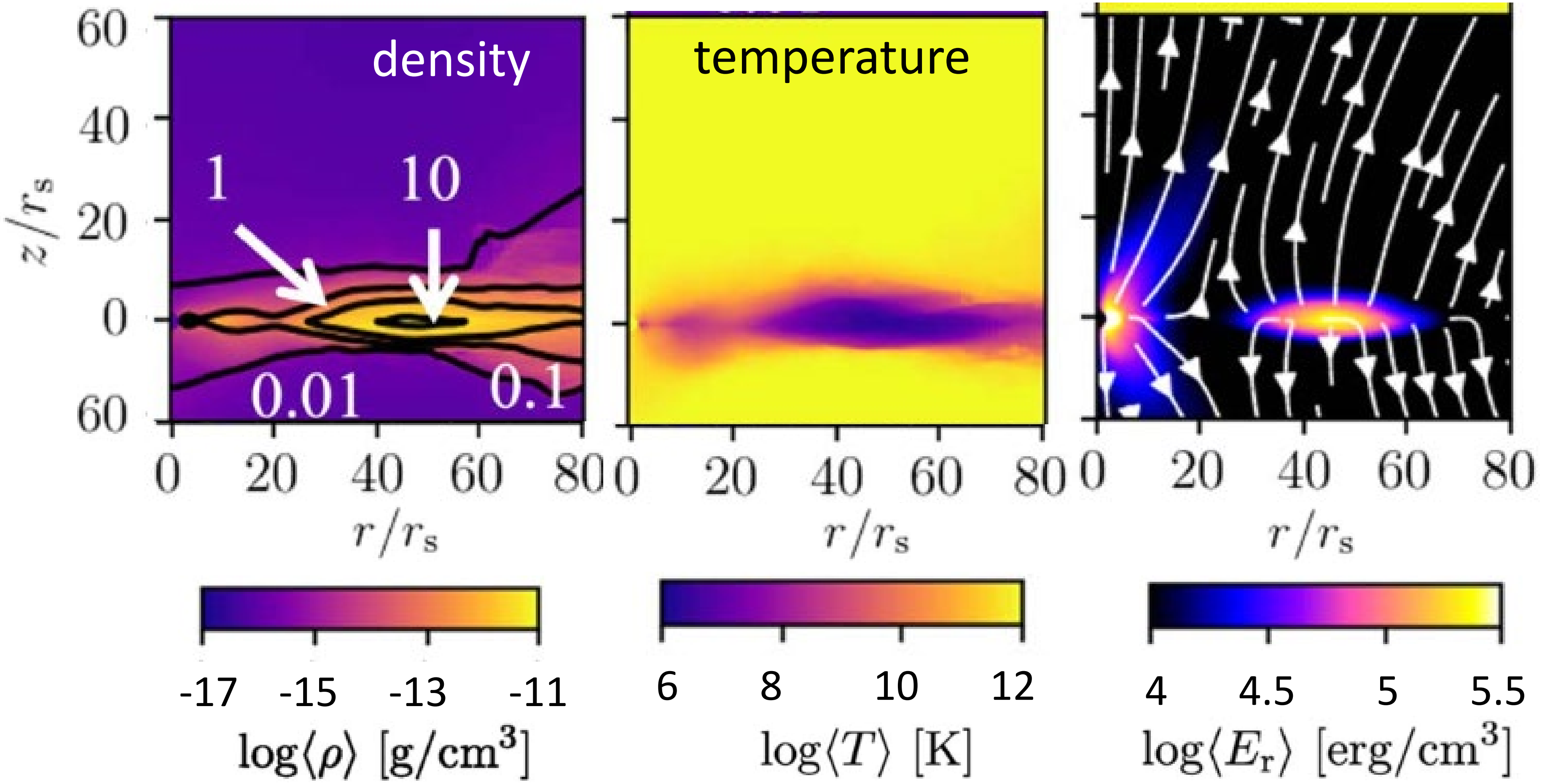

Igarashi et al. 2024

Formation of Low-β Region

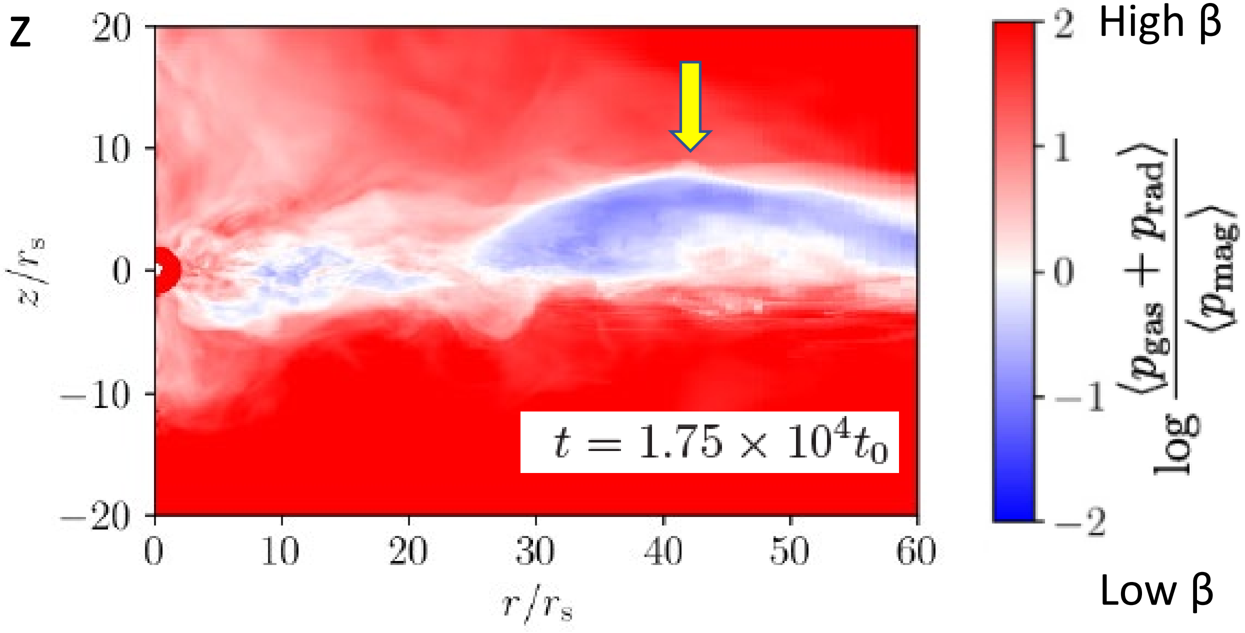

Ratio of
(gas pressure + radiation pressure)/
Magnetic pressure

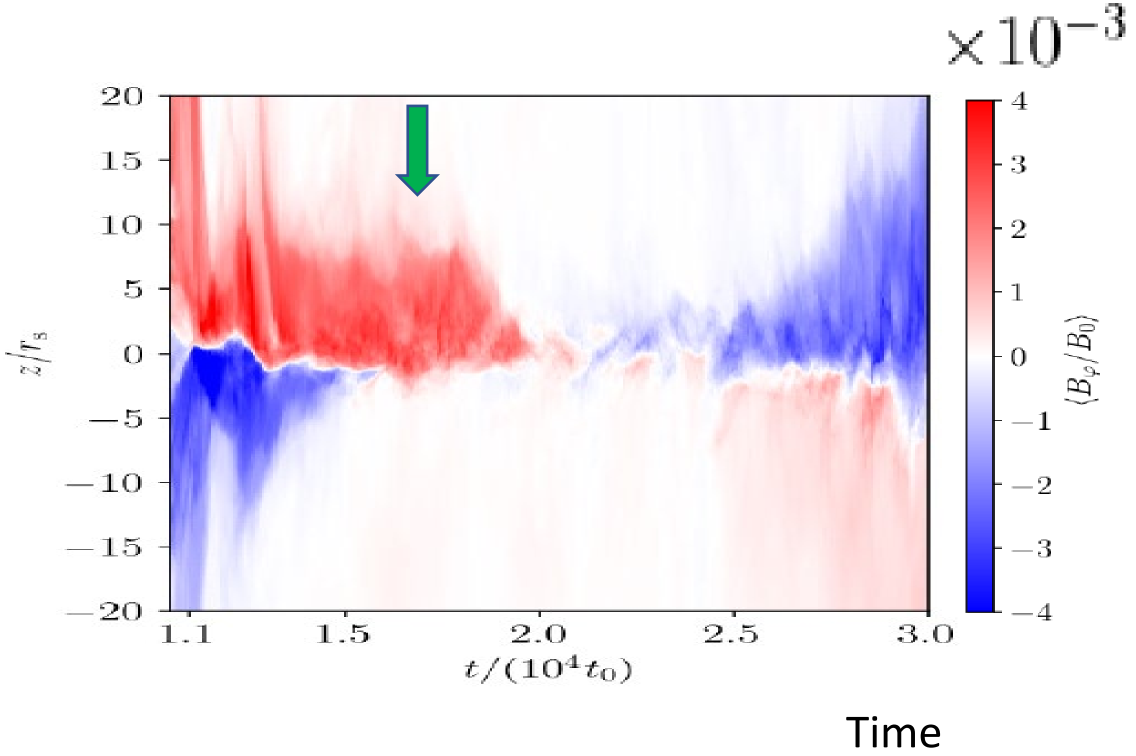

Butterfly Diagram of B_ϕ at $r=40r_s$

Magnetic Heating of the Warm Region

Vertically Integrated Magnetic Energy

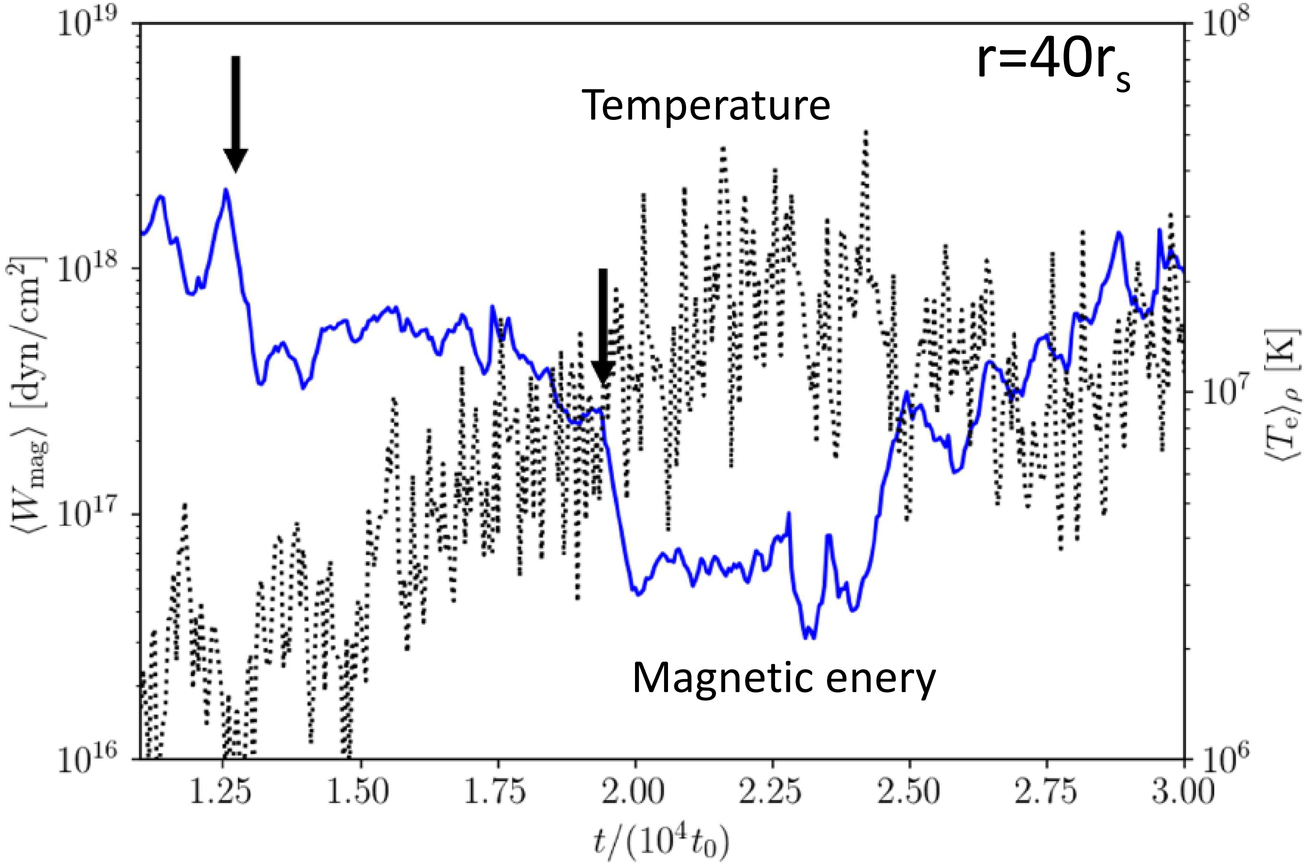

Time

Igarashi et al. 2024

Time Evolution of Toroidal Magnetic Field (Color) and Poloidal Magnetic Field (Solid Curves)

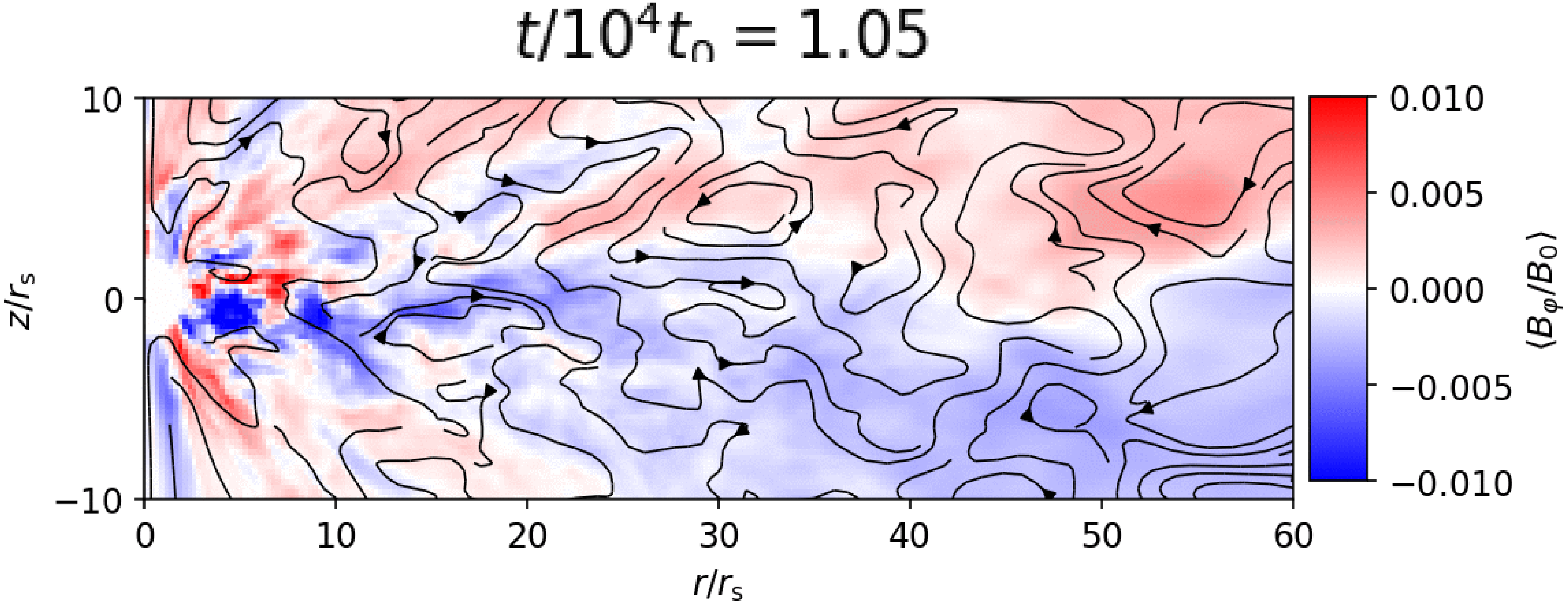

Igarashi et al. 2024

Merging of Toroidal Magnetic Flux Tubes

t /t_0= 1.3E4

t/t_0 = 1.4E0

t /t_0= 1.7E4

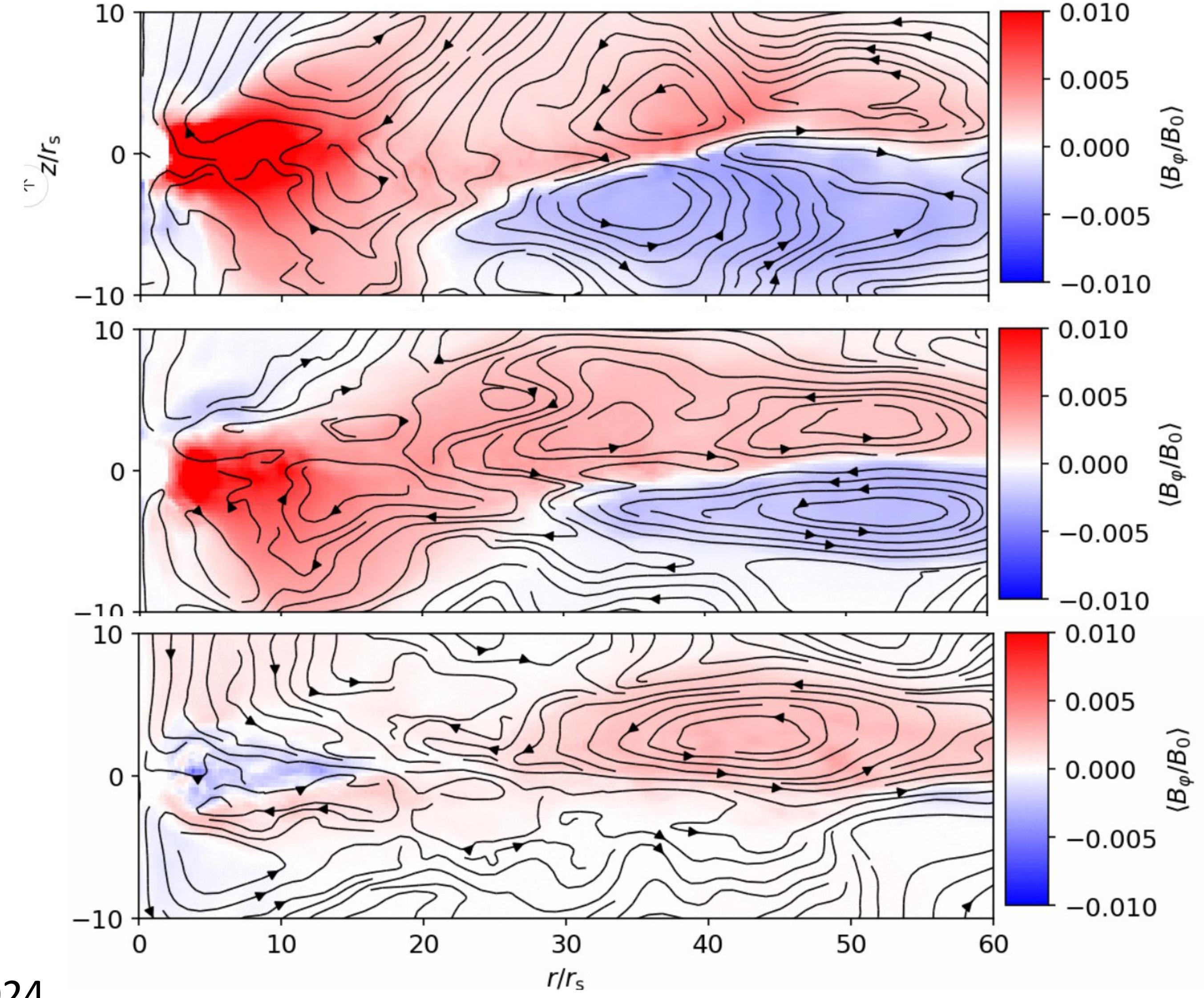

Igarashi et al. 2024

Similarity with the Merging of Spheromacs

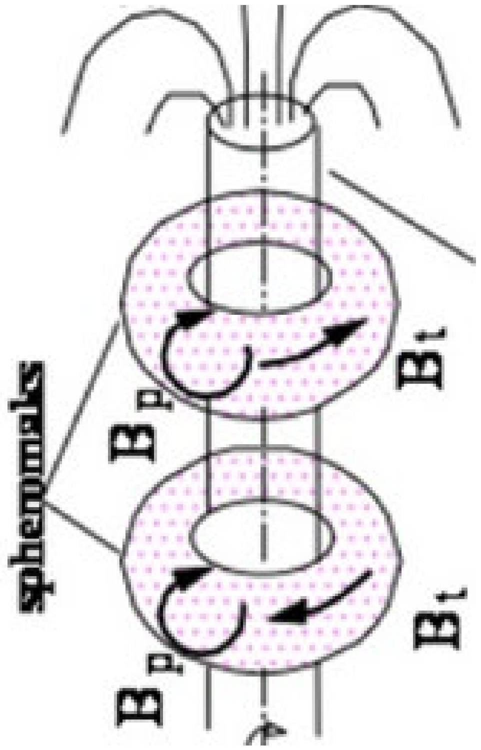

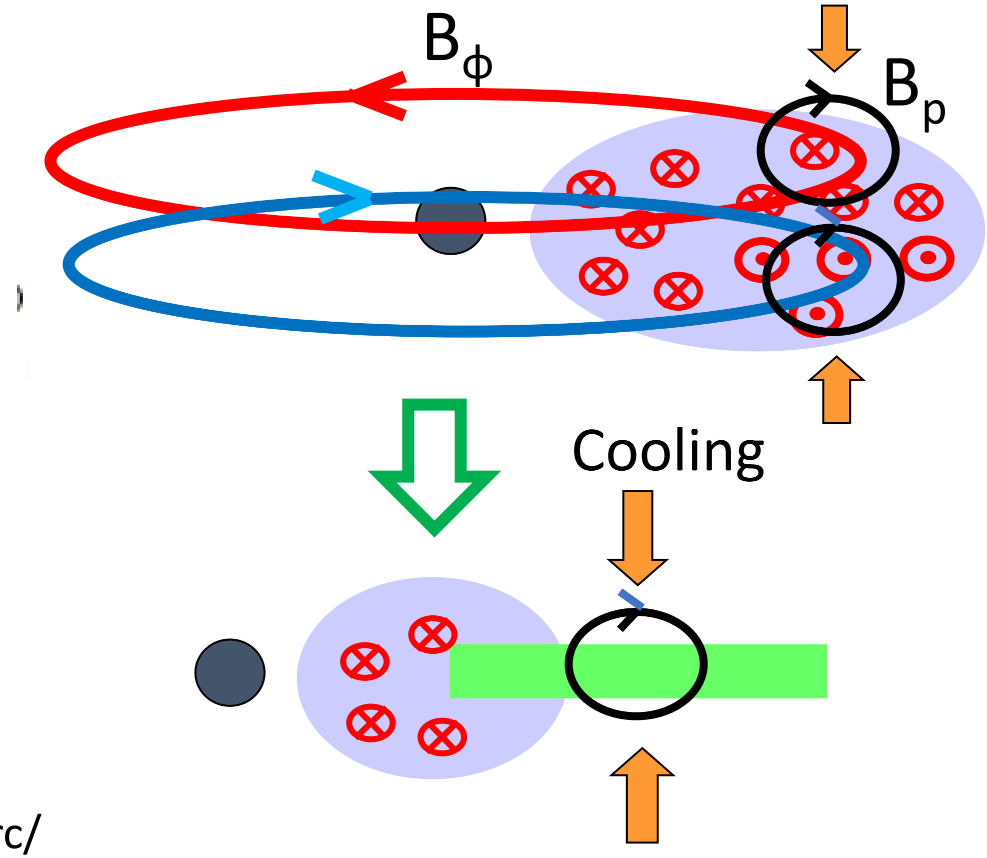

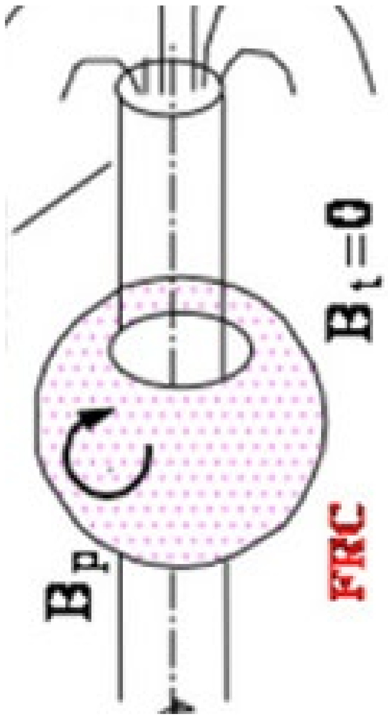

http://tanuki.t.u-tokyo.ac.jp/frc/

Comparison with Analytical Model

W $_{tot}$ r=40r$_s$ $\alpha = 0.1$ $\Phi_0 = 3 \times 10^{16}$ Mx/cm $\Phi = \int B_\varphi dz = \Phi_0 \left(\frac{\Sigma}{\Sigma_0}\right)^\zeta$ $\zeta = 0.5$

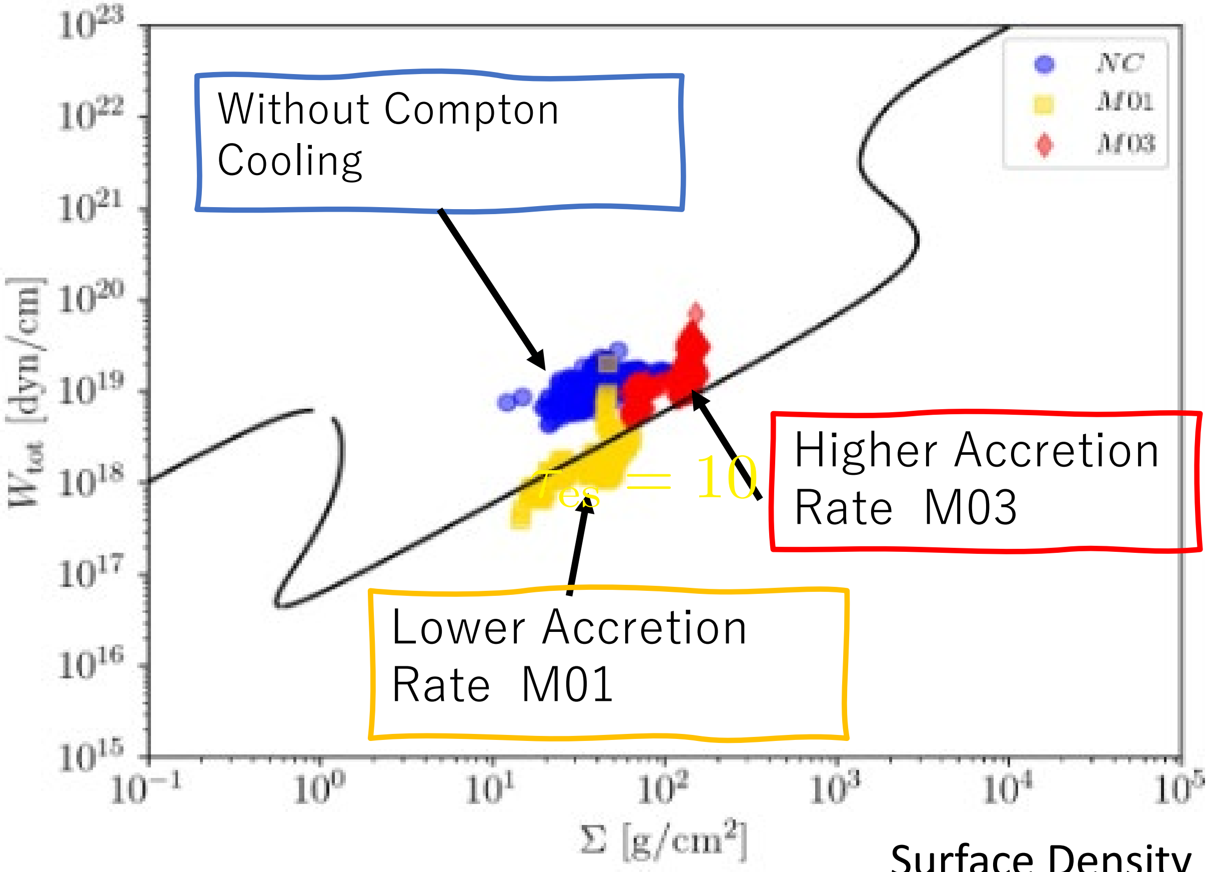

Surface Density

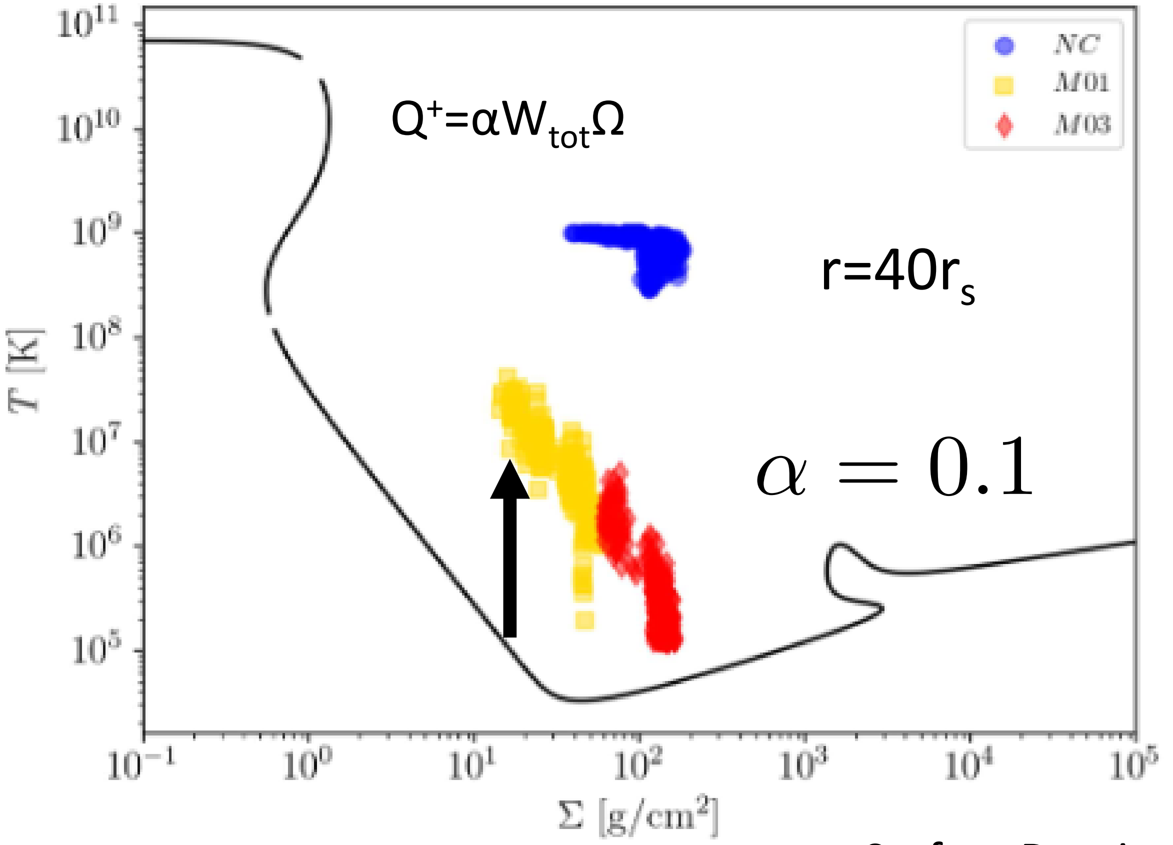

Surface Density

Igarashi et al. 2024

Transport of Poloidal Poynting Flux

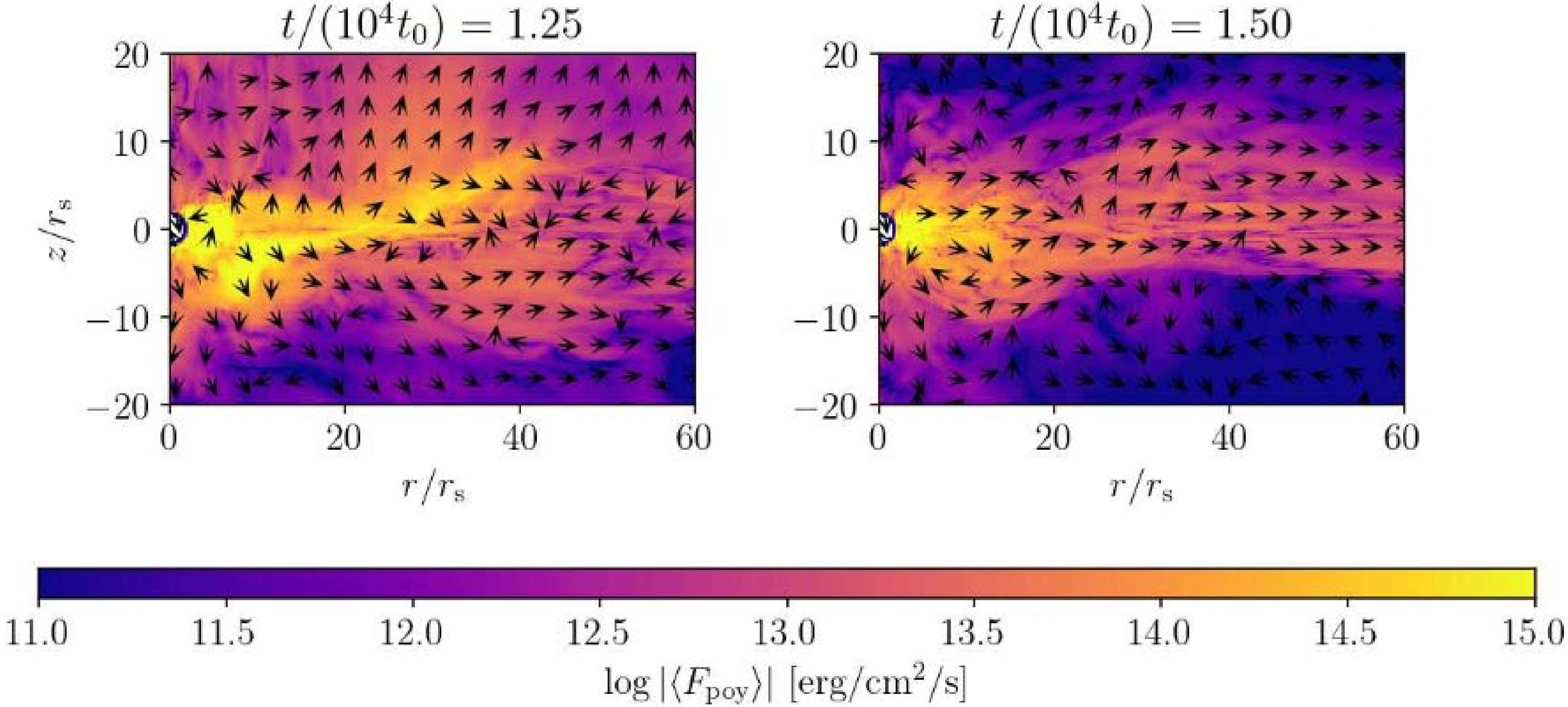

Igarashi et al. 2024

Updated Analytical Model

Mass Conservation $\dot{M} = -2\pi r \Sigma v_r = \mathrm{const.}$

Angular Momentum $\dot{M}\,(l - l_{\rm in}) = 2\pi r^2 \alpha W_{\rm tot}$

Total Pressure $W_{\rm tot} = W_{\rm gas} + W_{\rm rad} + W_{\rm mag}$

Energy Conservation $\frac{\dot{M}}{2\pi r^2} \frac{W_{\rm rad} + W_{\rm gas}}{\Sigma} \xi = Q^+ - Q^-,$

Heating (Q^+) Radiative Cooling (Q^-)

Classical Model $Q^+ = \alpha W_{\rm tot} \Omega$

Include Additional non-local Heating by Radial Poyinting Flux

$Q^+ = (\alpha + \alpha') W_{\rm tot} \Omega$

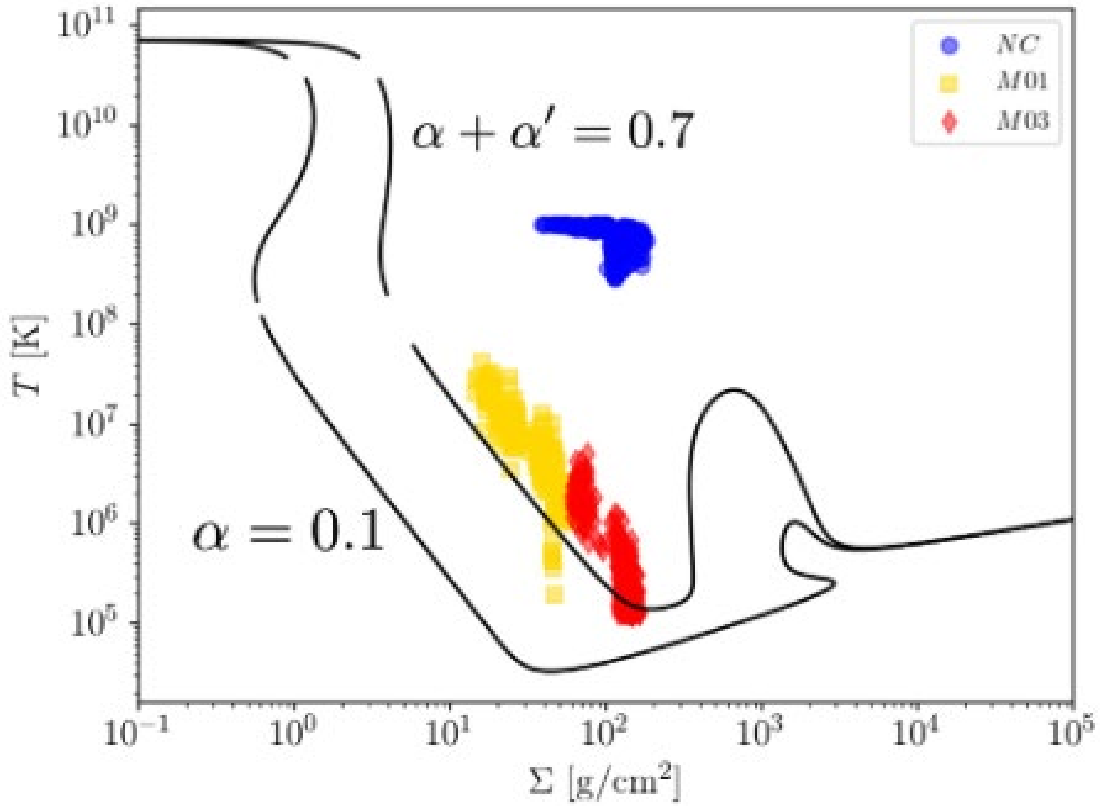

A Schematic Picture of Numerical Results

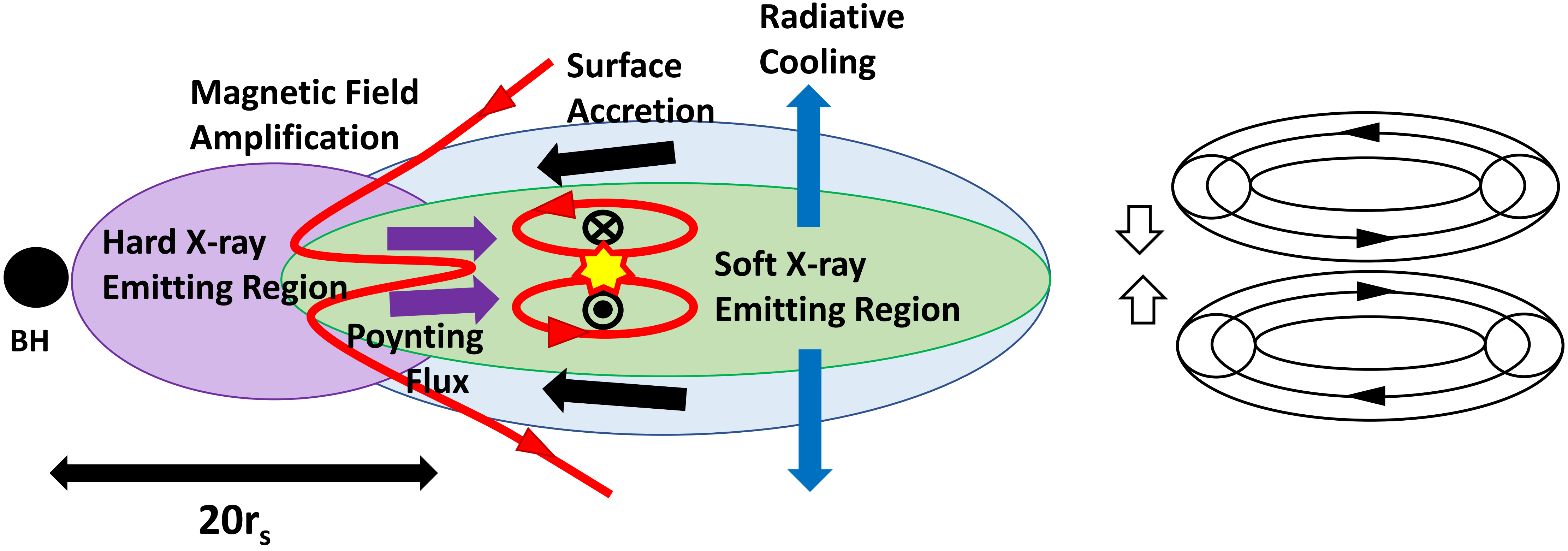

Summary

- Global three-dimensional radiation MHD simulations showed that during a hard-to-soft state transition, hard X-ray emitting hot radiatively inefficient accretion flow near the black hole co-exists with the warm, radiatively cooled disk.
- The radiatively cooled region becomes supported by magnetic pressure because azimuthal magnetic field is enhanced due to the vertical contraction of the disk by radiative cooling.
- The equilibrium temperature of the warm region is higher than the model of the magnetically supported disk by Oda et al. (2009). The enhanced heating is due to the radial transport of the magnetic energy accumulated around the interface between RIAF and the warm disk.
- The magnetic energy transported to the warm region is released by merging of helical magnetic flux tubes, and heats the disk.

Ion Heating by Merging of Spheromaks

Y. Ono, M. Yamada, T. Akao, T. Tajima, and R. Matsumoto   Phys. Rev. Lett. 76, 3328 (1996)

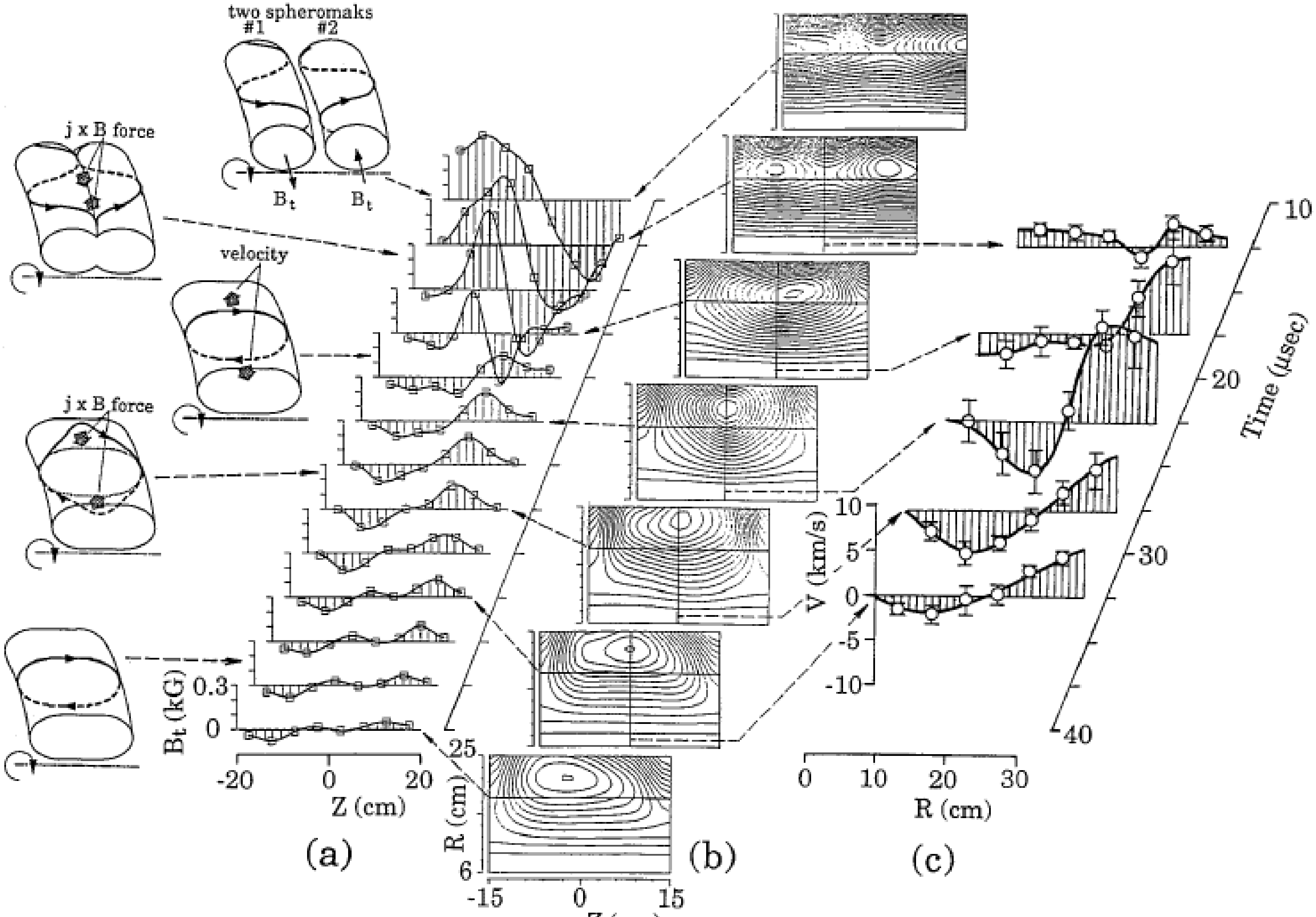

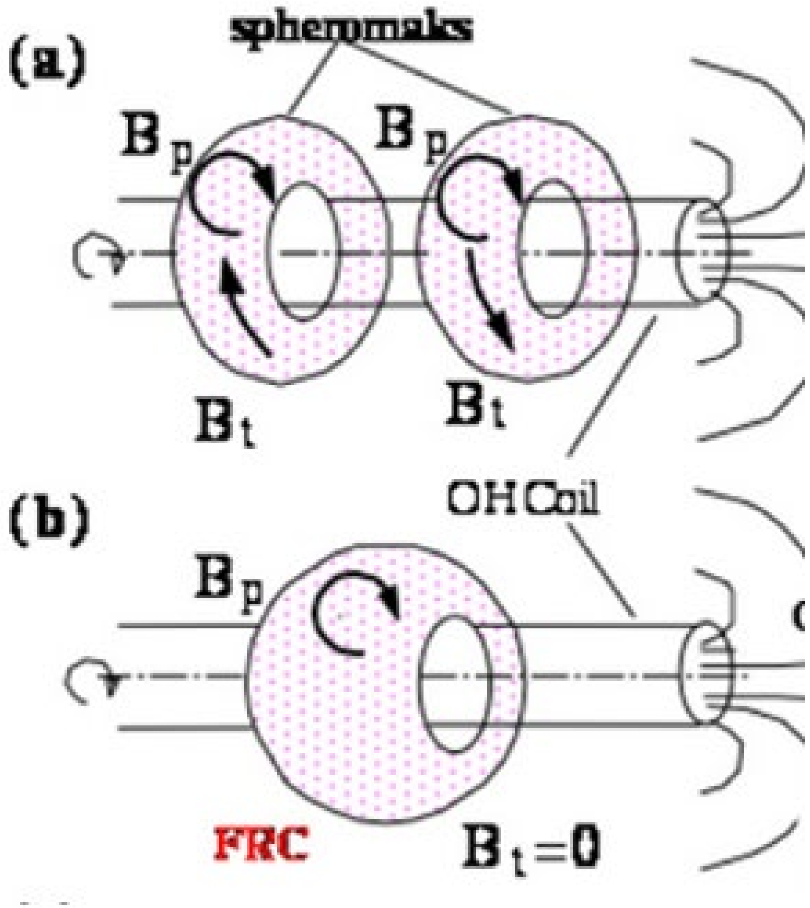

http://tanuki.t.u-tokyo.ac.jp/frc/

Than You for Your Attention !

Magnetically Arrested Disk （MAD）

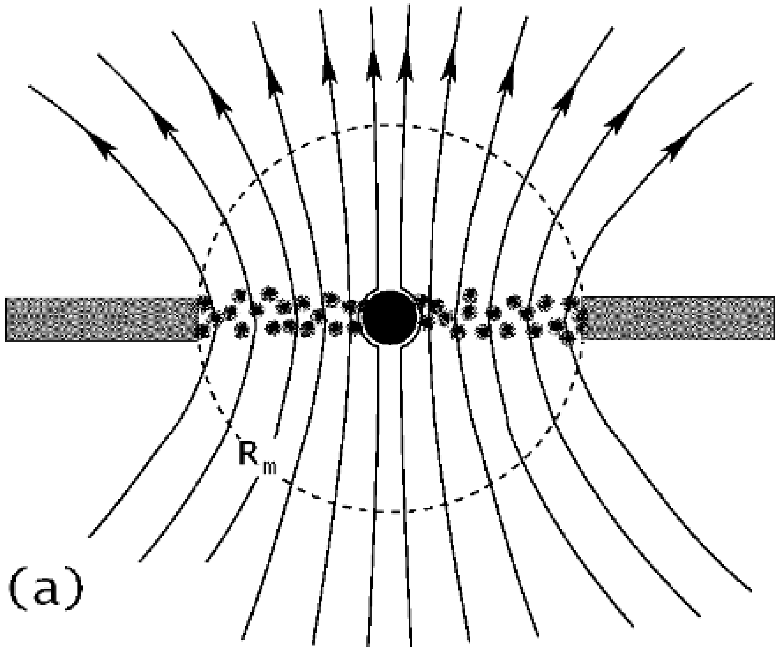

MAD

Narayan, Igumenshchev, Abramowicz,
PASJ 55, L69 (2003)

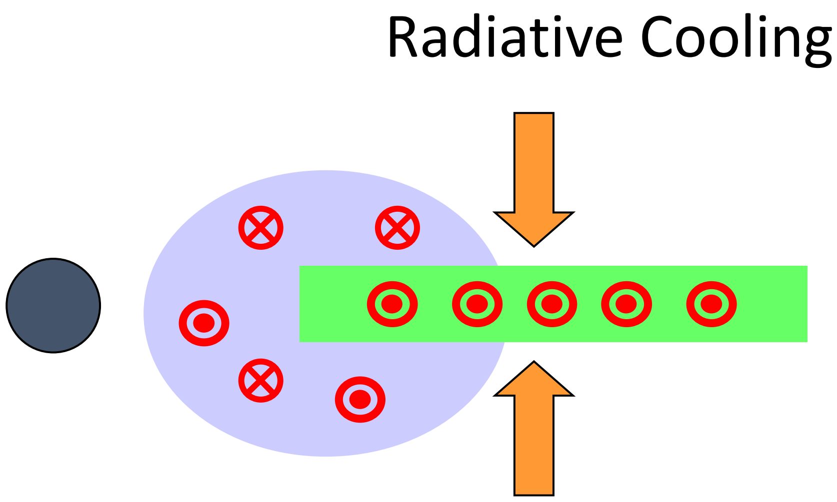

Toroidal
MAD ?

Machida et al. 2006

Two Faces of Active Galactic Nuclei

$L \sim L_{Edd}$

$L \sim 0.01 L_{Edd}$

High accretion rate

Low accretion rate

Quasar 3C273 (Chandra)

Seyfert Galaxy Mrk1018
(ESO/CARS survey)

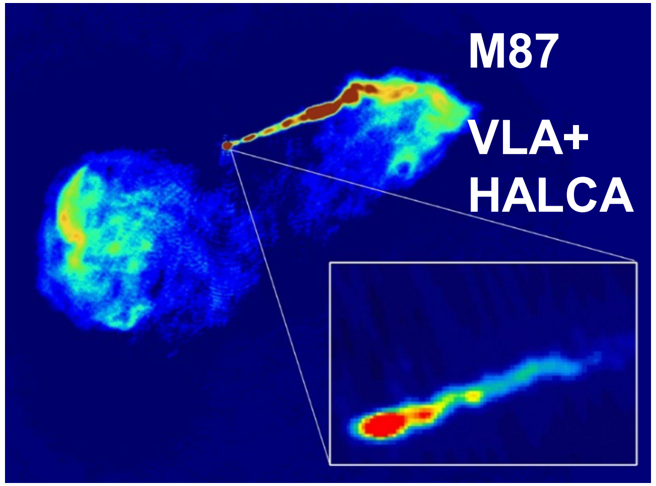

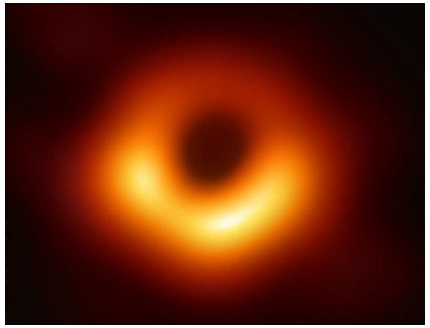

M87
EHT Collaboration
(2019)

Application of CANS+

Parker Instability

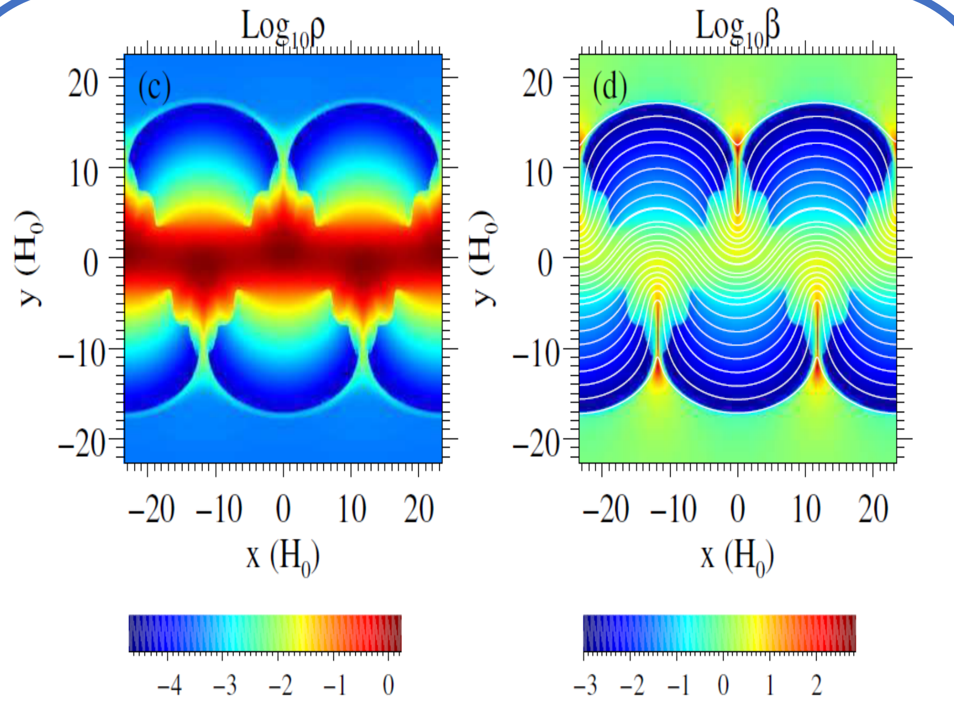

CANS+ can simulate
low-β region （$\beta = P_{gas}/P_{mag} = 10^{-3}$）

Magnetic Reconnection

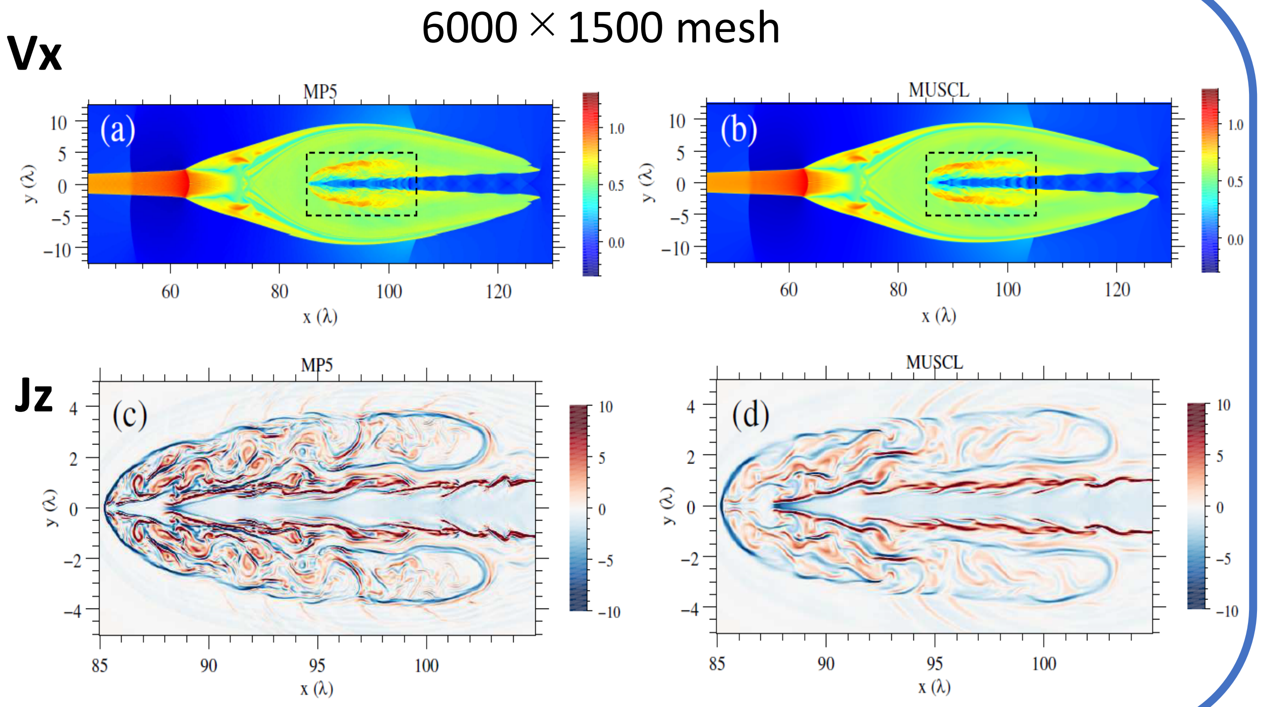

CANS+ can simulate magnetic reconnection and resolve shocks, discontinuities, and turbulence generated by MR

Time Evolution of Azimuthally Averaged Surface Density and Temperature

Surface Density

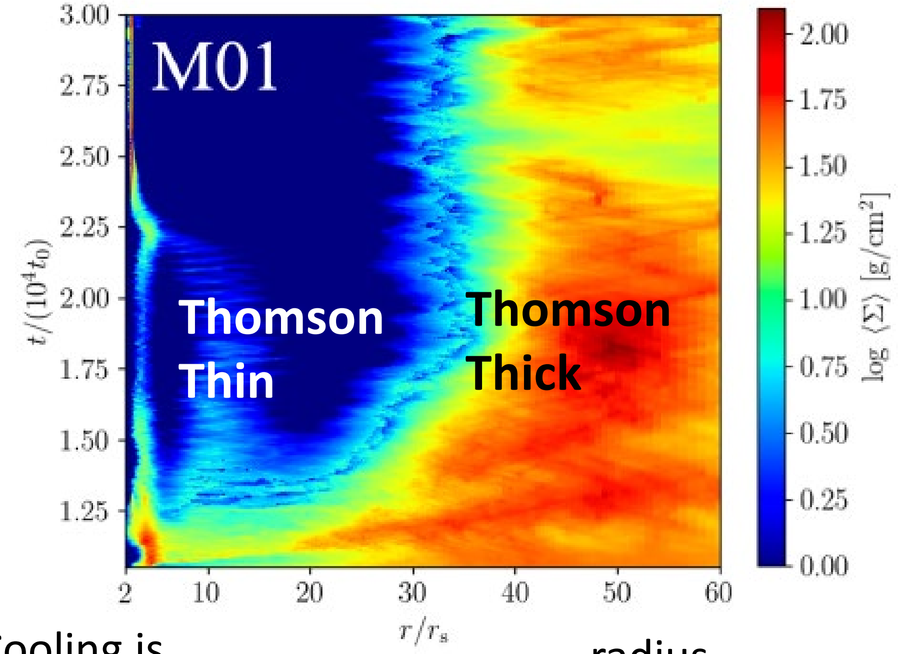

Cooling is Turned on

radius

Equatorial Temperature

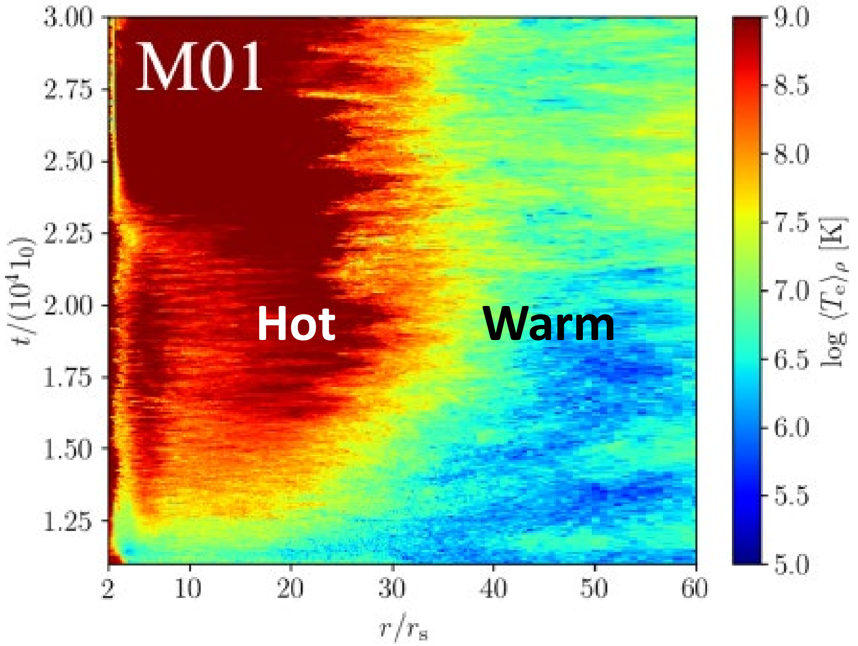

radius

Igarashi et al. 2024

Global Three-Dimensional MHD Simulations of Radiatively Inefficient Black Hole Accretion Flows

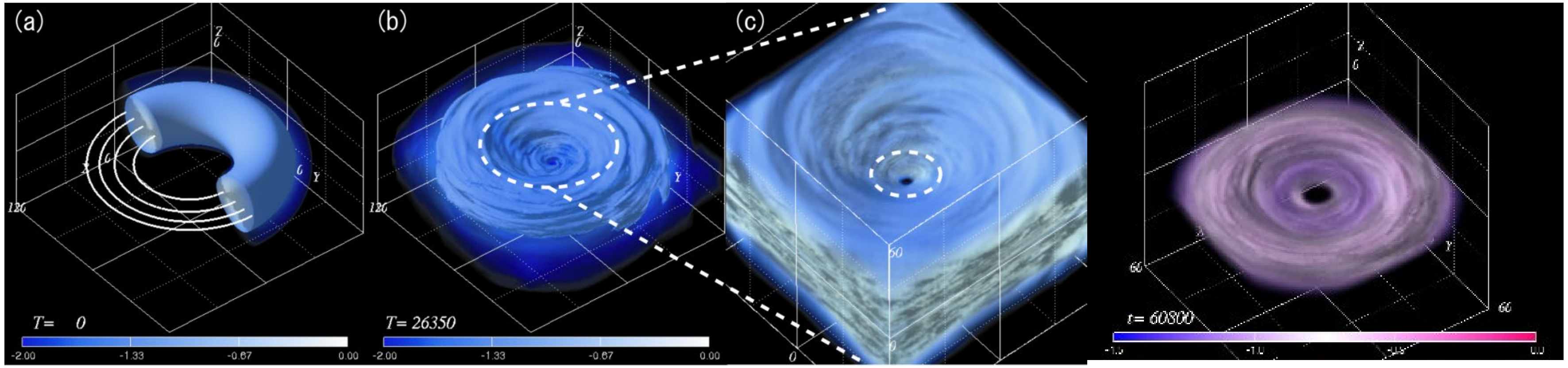

Machida et al. 2003

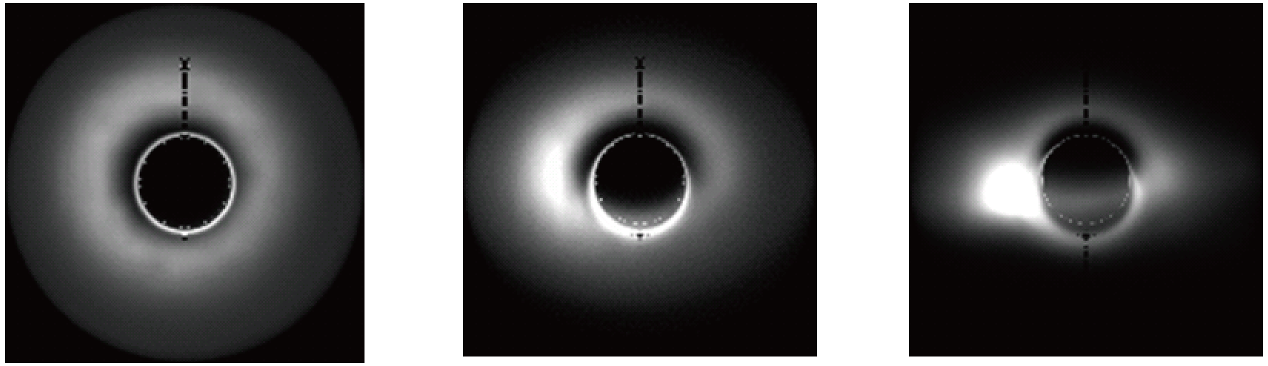

Machida, M. Bursa

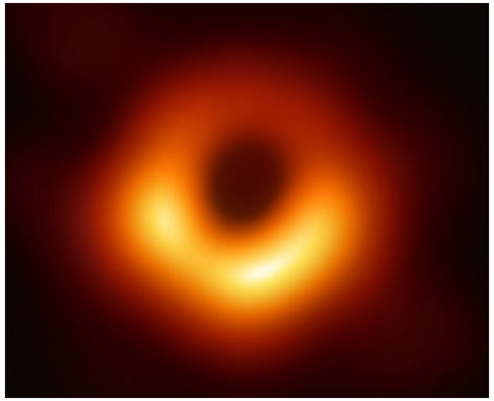

EHT Collaboration (2019)